THESIS FOR THE DEGREE OF LICENTIATE OF ENGINEERING

Antibacterial materials for wound care applications utilizing antimicrobial peptides

EDVIN BLOMSTRAND

Department of Chemistry and Chemical Engineering
CHALMERS UNIVERSITY OF TECHNOLOGY
Gothenburg, Sweden 2021

Antibacterial materials for wound care applications utilizing antimicrobial peptides

Edvin Blomstrand

Licentiatuppsatser vid Institutionen för kemi och kemiteknik
Chalmers tekniska högskola
Nr 2021:02

Department of Chemistry and Chemical Engineering
Chalmers University of Technology
SE-412 96 Gothenburg
Sweden
Telephone + 46 (0)31-772 1000

Cover: An illustration of a wound being exposed to bacteria with and without the presence of antibacterial material. A clear infection arises without the presence of the antibacterial material while the wound heals in a good manner with the antibacterial material present.

Printed by Chalmers Reproservice
Gothenburg, Sweden, Mars 2021

Antibacterial materials for wound care applications utilizing antimicrobial peptides

EDVIN BLOMSTRAND

Department Chemistry and Chemical Engineering

Chalmers University of Technology

Abstract

The spread of antibiotic resistance among bacteria has shown that the development of alternative treatments of infections is of vital importance. This thesis has looked at one potential candidate, antimicrobial peptides (AMPs), as an alternative or compliment to traditional antibiotics. AMPs are short peptides, normally just 10-25 amino acids long, that are part of our own innate immune system. Their mode of action to eradicate bacteria is most commonly by the disruption of the membrane of the bacteria. This mode of action makes it difficult for the bacteria to develop a resistance against AMPs, as it would require a fundamental change of their membrane structure. The challenge with using AMPs is their sensitivity towards proteolytic degradation when in a biological environment containing proteolytic enzymes. This thesis has used covalent attachment to a material as a means to increase this stability.

A wound bed is a haven for opportunistic pathogens and regardless of if it is caused by trauma or a surgical incision, bacteria that finds their way into a wound need to be dealt with in order to prevent an infection. Two approaches have been investigated in this thesis, with wound management as the application in mind. In the first approach, soft hydrogels were made out of the block copolymer Pluronic F-127 diacrylate. The polymer self-assembled into lyotropic liquid crystals which in turn were cross-linked in place. To these hydrogels, the antimicrobial peptide RRPRPRPRPWWWW-NH_2 was covalently attached. This resulted in a non-toxic material consisting of 90 wt% water with an antibacterial surface active against the clinically relevant strains of bacteria *S. aureus, S. epidermidis,* and *P. aeruginosa.* It also showed good antibacterial effect against the antibiotic resistant strains MRSA and MDR-*E. coli*. In addition, this method increased the stability of the peptides against proteolytic degradation in serum.

The second approach focused on the development of particles using the same material foundation as the first approach. Particles were chosen in order to increase the antibacterial potential as well as obtaining a material suitable for applications where a liquid formulation is desired. The produced particles had a high antibacterial effect both in solution as well as in a slurry. For the slurry, the bacterial load of *S. aureus* in an agar plate model was reduced by 99.99%. Cryogenic electron microscopy experiments indicated that the mechanism of action for the AMP-modified particles indeed was due to interaction with the bacterial cell wall/membrane.

Keywords: Antimicrobial peptides, hydrogels, self-assembly, lyotropic liquid crystals, antibacterial surface, Pluronic F-127

List of publications

Paper 1.

Antimicrobial Peptide Functionalized Mesoporous Hydrogels

Saba Atefyekta[#], Edvin Blomstrand[#], Anand K. Rajasekharan, Sara Svensson, Margarita Trobos, Jaan Hong, Thomas J. Webster, Peter Thomsen, and Martin Andersson

Submitted for publication

# These authors contributed equally to this work

Paper 2.

Cross-Linked Lyotropic Liquid Crystal Particles Modified with Antimicrobial Peptides for Antibacterial Applications

Edvin Blomstrand, Anand K. Rajasekharan, Saba Atefyekta, and Martin Andersson

Manuscript

Contribution report

1. Shared main author, performed all sample preparation, bacterial assays and MTT assay.

2. Main author, performed all experiments and analysis except for cryo-EM, and the FTIR, and Raman measurements.

Publications not included in this thesis:

Tough Ordered Mesoporous Elastomeric Biomaterials Formed at Ambient Conditions

Anand K. Rajasekharan, Christoffer Gyllensten, Edvin Blomstrand, Marianne Liebi, and Martin Andersson

ACS Nano 2020, 14, 1, 241–254

Acknowledgments

I would like to thank my supervisor Martin Andersson for all your help and endless source of ideas and solutions to the problems I encounter. My co-supervisor Anand K. Rajasekharan for all your support and for enlightening discussions. Saba Atefyekta for all your help with any microbiology concerns I have had. My Examiner, Hanna Härelind, for your time and effort regarding this work.

I would also like to thank all the members of MA research group for all the coffee breaks, lunch dates and intriguing discussions. Thank you for making every working day a joyous occasion. I would also like to thank everyone at the division of applied chemistry for providing a fun and welcoming atmosphere.

Furthermore, I would like to thank Camilla Holmlund at the Umeå core facility for electron microscopy for her assistance with capturing cryo-EM images of my elusive particles. Thomas Webster and his research group at Northeastern University, Boston, for giving me the opportunity to work in his lab. Chalmers Materials Analysis Laboratory (CMAL) for assistance with Fourier transform infra-red spectroscopy and Raman spectroscopy. And Jenny Perez Holmberg for her assistance with the dynamic light scattering measurements.

Finally, I would like to thank my girlfriend Astrid for your seemingly endless love and moral support. Also thank to our dog Novi for your ability to put a smile on my face even on the gloomiest of days.

Abbreviations

AMP	Antimicrobial peptide
CFU	Colony forming units
Cryo-EM	Cryogenic transmission electron microscopy
DA-PF127	Diacrylated Pluronic F-127
DLS	Dynamic light scattering
EDC	1-Ethyl-3-(3-dimethylaminopropyl)carbodiimide
FTIR	Fourier transform infra-red
LLC	Lyotropic liquid crystal
MDR-*E. coli*	Multi-drug resistant *Escherichia coli*
MIC	Minimum inhibitory concentration
MRSA	Methicillin resistant *Staphylococcus aureus*
NHS	N-hydroxysuccinimide
PBS	Phosphate buffered saline
SAXS	Small angle X-ray scattering
TEM	Transmission electron microscopy
TSB	Tryptic soy broth
UV-vis	Ultraviolet-visible

Table of Contents

1. Introduction

The human body is a marvelous thing, consisting of trillions of individual microscopic cells that are working in unity to achieve movement, thinking, digestion, defense, and a number of other features. It even has the ability to repair itself: when DNA does not get copied correctly there are enzymes that repair it [2]. When trauma causes blood vessels to rupture and form bruises, the cells in the body stops the internal bleeding and rebuild the blood vessels [3]. But the human body is not perfect. Sometimes things go wrong to such an extent that the repair system cannot handle the damage and needs help. If the DNA damage for example becomes too severe for the body to handle, it can lead to tumor formation, which can have a devastating effect. If an acute trauma is so great that a large wound is formed, the body might not be able to stop the bleeding by itself and might not be able to heal the wound without some assistance. Luckily, millennia of development of healthcare and medicine has done wonders for treating both disease and acute trauma. Humans have never had a higher life expectancy than today, and a number of earlier untreatable conditions are now treatable. Some diseases have even been eradicated. One thing that has been crucial for this progress is antibiotics. Bacteria have been present throughout our history, causing infections that have been killing people and impairing peoples' lives. When breaches of the skin or other defense systems of our bodies are too large, bacterial infection can arise. Antibiotics have made it possible to treat these conditions effectively in ways that were not possible before. However, the emergence of antibiotic resistant bacteria is threatening to nullify this development. Alternatives to antibiotics are therefore in high demand, and one promising alternative is antimicrobial peptides.

The aim of this thesis was to evaluate the incorporation of antimicrobial peptides to soft hydrogels for applications within wound care. Two approaches (illustratively shown in Figure 1) were taken for this:

- Soft hydrogel sheet made from non-toxic polymers self-assembled into lyotropic liquid crystals that were then cross-linked into shape. Antimicrobial peptides were then covalently attached to the surface of these lyotropic liquid crystals. Potential application for this could be as a wound dressing.

- Particles made of lyotropic liquid crystals post-modified with antimicrobial peptides. Compared to sheets, particles were prepared to get a higher antimicrobial surface while also gaining the potential of an antimicrobial liquid formulation.

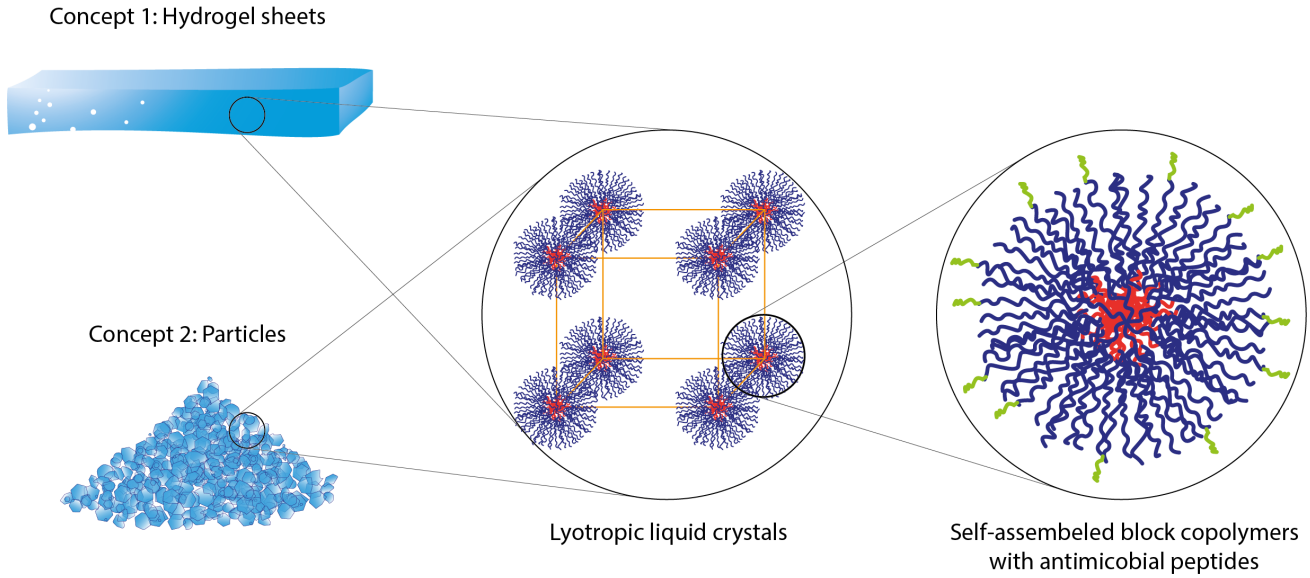

Figure 1. The two concepts used in this thesis to produce antibacterial materials. Both the hydrogel sheets (top left) and the particles (bottom left) are built up by amphiphilic polymers that have self-assembled into a micellar cubic phase (middle). The sheets and particles were subsequently cross-linked into shape and modified with covalently attached antimicrobial peptides (far right). The red in the structure represents the hydrophobic polypropylene oxide region of the polymer, the blue represents the hydrophilic polyethylene oxide region of the polymer, and the green represent the antimicrobial peptides.

2. Background

To better understand the concept of this thesis, I have broken down the background into four sections depicting the ongoing battle that the cells in our bodies are going through against the elements of our surroundings.

2.1. The battleground

Our bodies most important defense system is also our largest organ, the skin. It consists of several layers which each has its own unique function. Outmost, at the very surface, we find the epidermis, consisting almost completely of a monoculture of keratinocytes. The keratinocytes proliferate from basal cells and then goes through cell differentiation, in which they become highly ordered while also forming tight junctions which connects them tightly to each other [4]. They also produce keratin, which together with the cells and an extracellular lipid layer form a layer that works as a barrier towards even the smallest molecules [5]. This helps containing water and heat inside of our bodies while keeping pathogens out.

Beneath the epidermis lies the dermis. This layer consists of connective tissue built up by structural components like collagen, elastin, and hyaluronic acid. This gives the skin its elasticity and cushions the body somewhat [6]. Hair cells, heat receptors, nerve cells and blood vessels are also found in the dermis. The major cell groups found here are fibroblasts, whose main function is to synthesize the extracellular matrix components [7]; macrophages, whose main function is to neutralize threats if a breach in the epidermis is formed [8]; and mast cells, whose main function is to activate the immune system when a threat is detected, but also to activate wound healing [9].

Beneath the dermis lies the subcutaneous tissue. Its function is to connect the layers above to underlying muscle and bones and consists of connective tissue along with fat cells [10]. The subcutaneous tissue also cushions the internal organs and provides some insulating effect.

With this in mind, it is apparent that damage to the skin can result in several serious conditions. The first noticeable thing is that blood will be pouring out if blood vessels are ruptured. In major trauma this can lead to exsanguination. Higher degree burns can cause damage to the dermis so severe that it results in a permanent loss of sensitivity, inability to control body temperature and inability to prevent water loss through evaporation [11]. Damage to the skin will also give pathogens access to internal parts previously protected. However, as mentioned before, the body has the ability to repair itself, and wound healing is a well-oiled machinery. Generally, the wound healing is broken down into four stages: coagulation, inflammation, proliferation, and remodeling. The most acute problem to deal with is to stop the bleeding, which is what the coagulation does. Through platelet activation and fibrin formation, blood clots are formed, which effectively clogs up the bleeding [12]. The next stage is inflammation, which deals with cleaning up the wound. This is done by leukocytes, which remove debris,

clear out damaged tissue and cells, and deal with potential pathogens [13]. Some leukocytes also release cytokines which attract other cells to the site in order to start the third stage: proliferation. In this stage the tissue is built up again: blood vessels are formed by angiogenesis [14], connective tissue is produced by fibroblasts, and the epidermis is formed by epithelial cells migrating into the non-covered area [15]. The final part is the remodeling of the wound, where unnecessary cells are removed, and the collagen is remodeled into stronger bundles [16].

Due to this well-tuned wound healing process, most drugs and medical devices try not to interfere with the wound healing but instead try to optimize the conditions for its function. One of the most important features of any kind of wound dressing is to replace the broken barrier that provide shelter from the outside [17]. Having an external barrier also helps keeping the wound moist by hindering evaporation. This is why even the simplest plaster can be quite effective at giving a wound a good environment for healing. More extensive wounds, however, can have a trickier time healing in a good way, and more advanced help might be required. If a child falls and scratches up their knee for instance, there most likely will be dirt or gravel in the wound. Manual debridement of such wounds will help the healing significantly while also lowering the risk of pathogens gaining access to the underlying tissue. For deep gashes, the healing can be greatly helped by stitching the wound together (after debridement, if necessary), which will put things back in place while also covering up the wound and minimizing the gap that needs to be healed. For large burn wounds, soft hydrogels or hydrocolloids with a high water content can be used. These have shown to give pain relief for patients while also giving the wound a moist environment, which improves healing rate significantly [18].

There are a high variety of dressings designed for various types of wounds. Some dressings even incorporate active substances aimed at enhancing certain aspects of the wound healing process. The substances could be antimicrobials, aimed at preventing microbial organisms from infecting the wound [19-21], it can be growth factors, aimed at increasing certain activity of certain cells [22, 23], or it can be supplements, aimed at providing the cells of the wound healing process with everything they need in order to do their best job possible [24, 25].

2.2. Invading forces

As mentioned before, a lot of the functions of the skin and wound management involves protection from microbes, and there is a good reason for this. Microbes are an ancient form of organisms, speculated to have been the very first form of life found on earth. And they are ever-present. They exist in numerous forms and at all places on earth. Most important for this thesis are bacteria. Bacteria sometimes gets a bad reputation, but under normal conditions they are great allies of humans. We have an extensive flora of microbes in our guts for instance – consisting mainly of bacteria – called the gut microbiota. The human body serves as a host for the microbiota, providing it with a steady flow of nutrients, and the microbiota are metabolizing nutrients that our own cells cannot deal with on their own. The microbiota even synthesize important elements that we need to function properly but cannot synthesize by ourselves [26]. Bacteria are also present on our skin, and each human has their own flora of bacteria. The

bacteria found on the skin are normally not harmful and can even provide some benefits for us by essentially keeping the harmful bacteria away [27].

However, when a breach in the skin barrier occurs, bacteria can find their way into the wound bed and that is a different story. What has kept microbes around all these years is their fantastic ability to adapt to new situations. When a new environments appears, bacteria will try to take advantage of the change and colonize the environment, especially a habitat as cozy and rich in nutrients as a wound bed [28]. This kind of process is called an opportunistic infection. It therefore does not come as a big surprise that the bacteria most commonly found in wound infections are also bacteria found in our normal skin flora [29-31].

Our bodies have several mechanisms to combat intruding bacteria. Directly after a breach and pathogenic invasion there is a rapid response that is non-specific and broad-spectrum. This is part of the innate immune system. The cells that are part of the innate immune system will try to neutralize intruding pathogens by lysing them, ingesting them, or kill infected cells [32, 33]. During this process they will also gather information about the intruding pathogens, and by gathering the antigens specific to the pathogen, the adaptive immune system can be activated [34]. The adaptive immune system can target specific pathogens more effectively by the use of antibodies that are sensing the antigens specific to the pathogen. By saving these antibodies in specific memory cells, the adaptive immune response towards specific pathogens can be quicker and elevated for the next time the same pathogen invades the host.

However, if the microbial load is too high, or if the immune system is compromised, it might lead to an infection that needs external help. Luckily, almost 100 years ago, arguably the most important discovery for modern medicine was discovered: penicillin, the first antibiotic. Antibiotic is a term for substances that are used in medicine to treat bacterial infections. The mechanism for antibiotics is very diverse but generally it inhibits a very specific function in the bacterium that can either kill it or stop its growth [35]. The positive thing with this specificity is that it can be very effective and still not harm human cells. The negative thing with the specificity is that changes in the targeted site will render it useless. This means that mutations in the bacterium DNA can make the bacterium resistant to certain antibiotics [36]. By removing antibiotics by specific efflux pumps from the inside of the bacterium to the outside or by hydrolyzing parts of the antibiotics, bacteria can also lower the concentration to none-lethal levels [36]. This causes what is known as antibiotic resistance. Whenever a new antibiotic has been introduced, it has not taken long before resistant strains have been found. Due to bacteria's ability to perform horizontal gene transfer, even between species, resistance can and have spread to the extent that some infections are again untreatable [37]. It is therefore of utmost importance to find alternatives or compliments to antibiotics. For instance, one of the oldest known antimicrobial agents is honey, and in some forms, it is still used in medicine today. Compounds in honey have shown to reduce microbial growth while also aiding the wound healing [38, 39]. However, the antibacterial effect is not that great when compared to other alternatives and producing honey in large quantities can prove difficult. Another compound that has been used for a long time in order to deal with bacterial infection is ionic silver. Today it is mainly used as nanoparticles and it is a highly effective antibacterial substance [40]. It has been incorporated into wound dressings, ointments and even textiles [21,

41, 42]. However, there is an ongoing discussion regarding the toxicity silver has towards mammalian cells [43, 44]. Moreover, silver needs to be eluted into the media where the bacteria are found, which limits its applications.

2.3. The (potential) savior

One promising alternative to traditional antibiotics is antimicrobial peptides (AMPs). These are short chains of amino acids, normally just 10-25 amino acids long. AMPs have been used to combat bacterial infections for millennia, since they are a part of the innate immune response of a lot of organisms, ours included [45]. They exist in a large variety of structures and they can also target different components of the bacteria. What differentiate them from antibiotics is that they target a general structure and not a specific site, which means that resistance is much more improbable [45, 46]. The target for AMPs is generally the cell wall or the outer membrane of the bacteria [47], which makes resistance even more difficult to evolve since efflux pumps would be useless. This mechanism also gives the AMPs their specificity towards bacteria, since both gram negative and gram positive bacteria have negatively charged surfaces due to the lipopolysaccharides in gram negative bacteria and the teichoic acid in gram positive bacteria [46]. AMPs therefore generally have a positively charged section and a hydrophobic section. The secondary structure is usually an alpha-helix, which is sometimes formed by structural changes first when the peptide comes in contact with a membrane [48]. This gives the AMPs an attractiveness towards the negatively charged bacterial surface that it does not have towards the neutrally charged surface of the majority of mammalian cells. The peptides are suggested to exert their antimicrobial effect by forming pores in the membrane or by disintegrating parts of it in a surfactant-like manner [46, 49].

The main reason AMPs have not had a bigger impact in medicine is that they are very sensitive to proteolytic degradation [50]. This means that they have a very short life span once they are inside our bodies. This is fine if there are leukocytes around to continuously deliver a supply of peptides [51], which will also provide a local treatment. But it poses real difficulties for the incorporation into treatment options. There have been a few different approaches to deal with this issue throughout the last decades. Some research has been made to modify the base structure, where the amino acids has been changed from the regular L-configuration to the less commonly found D-configuration [52]. This will protect the peptides since the reaction siters on the enzymes that perform the proteolysis can normally only target the L-configuration. Others have tried to incorporate it into drug delivery systems which protects the peptides until they are released [53, 54]. The method used in this thesis is to bind the AMPs to a surface. By having the peptides bound to a surface it is hypothesized that this will sterically hinder the enzymes from gaining access to the cleaving sites, which in turn means that the AMPs can last longer in biological solutions containing proteolytic enzymes. There are several ways of doing this, and depending on the base material one has, different chemistries can be used. Important to keep in mind is that some studies have shown that some peptides lose their activity when bound to a surface [55, 56]. Also, the activity of some peptides can be strongly dependent on the inclusion of a spacer between the base material and the peptide [56, 57]. Furthermore, the orientation of the peptide while attached to the surface might also affect the potency of the antibacterial effect [58, 59], and should therefore be taken into consideration. It is of course of

outmost importance to also pick a peptide that does not need to get access to the intracellular matrix to exert its antibacterial effect. Due to these reasons, in this thesis, the AMP of choice is a synthetically made one with the structure RRPRPRPRPWWWW-NH_2. The structure for this can be seen in Figure 2. This peptide is very short with a heavily charged section and a section that is very hydrophobic. The secondary peptide structure is unknown but due to the short length, high proline content, and localized sections, any complicated structure is unlikely. The carboxyl group on the C-terminal has been blocked off by forming an amide group, giving the peptide an overall charge of +6 at physiological pH. In this thesis, the attachment is done by EDC/NHS coupling, which means that the primary amine group at the N-terminal is covalently attached to a carboxylic acid group found at the base material. This results in a zero-length conjugation, meaning that there is no additional spacer between the material and the peptide.

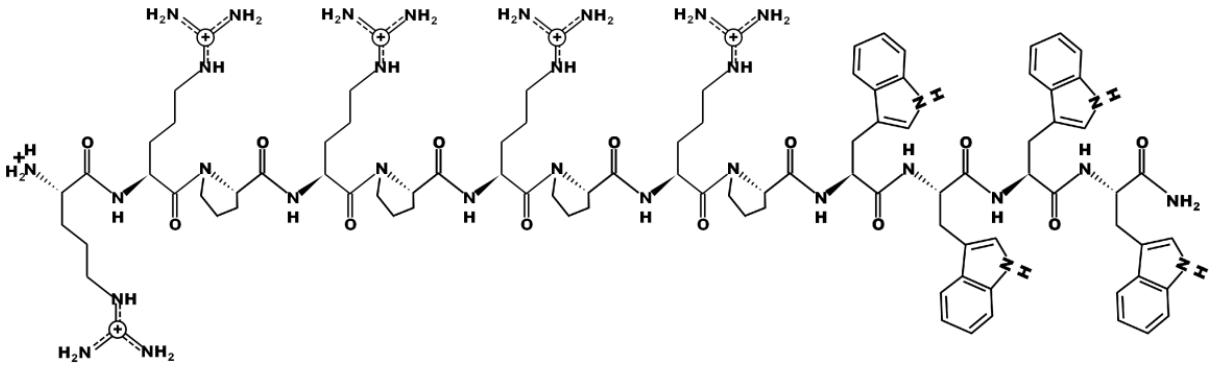

Figure 2. The structural formula at physiological pH of the synthetically produced antimicrobial peptide used in this study. The peptide consists solely of arginine, proline and tryptophan and the C-terminal have been modified to end on an amide group.

2.4. Presenting the savior

Depending on the application, the material foundation can be tuned to match the desired properties. In this thesis, a soft hydrogel with available carboxyl groups was desired in order to have a site for the AMP modification, as well as being comfortable if turned in to a wound dressing. For the synthesis of the hydrogel, the triblock copolymer Pluronic™ F127 was chosen, since it is regarded as not toxic, is FDA approved for some uses *in vivo* and is easily functionalized [60-62]. Furthermore, Pluronics have an amphiphilic structure and function as polymeric surfactants that self-assemble into lyotropic liquid crystals (LLCs) in solution (illustrated in Figure 3b) [1]. This means that the structure can be fine-tuned by changing concentration and type of solvent, as shown in Figure 3a. By modifying the ends of the Pluronic with the addition of acrylate groups, the LLCs can be cross-linked into place by exposure to UV radiation (with the addition of a photo-initiator). By further exposure to UV radiation or by simple hydrolysis, the formed ester bonds can be broken down to the desired carboxylic acids [63, 64]. Cross-linking will occur between the endpoints of the Pluronic molecules, which will be located at the outer points of the LLCs. It is therefore likely that the formed carboxylic

acid groups also will be located here. This means that the EDC/NHS will attach the AMPs mainly to the outer parts of the structures as illustrated in Figure 4.

F127 is one of the Pluronics with the highest hydrophilic portions, and in polar solvents this results in 'normal' phases with the hydrophobic parts tucked away inside the structures, illustrated in Figure 4. This opens up for the potential of loading the system with for example pharmaceutics for drug-delivery [65, 66]. Non-polar molecules can be loaded into the hydrophobic parts of the structures and polar molecules can be loaded into the hydrophilic parts of the structure. The release profile will be a bit different depending on where drugs are loaded, with a bigger initial burst of release from the hydrophilic section. Furthermore, when cross-linked into a hydrogel, the material should be able to swell by taking up water while still retaining the highly ordered structure. A wound dressing made out of this high water content material is suitable for wounds to keep them moist, which improves wound healing and increase the comfort for the wearer [18]. This kind of material is, however, not suitable for wounds with heavy exudate, since this might lead to maceration [67]. Furthermore, Pluronic shows no negative effect on mammalian cells in a 5% w/w solution, indicating that potential residues or applications in the blood or tissue can be performed in a non-harmful manner [68]. Further benefits from using Pluronic is that it is synthetically produced, meaning that it is easy to make in a scalable manner, which makes it more cost effective.

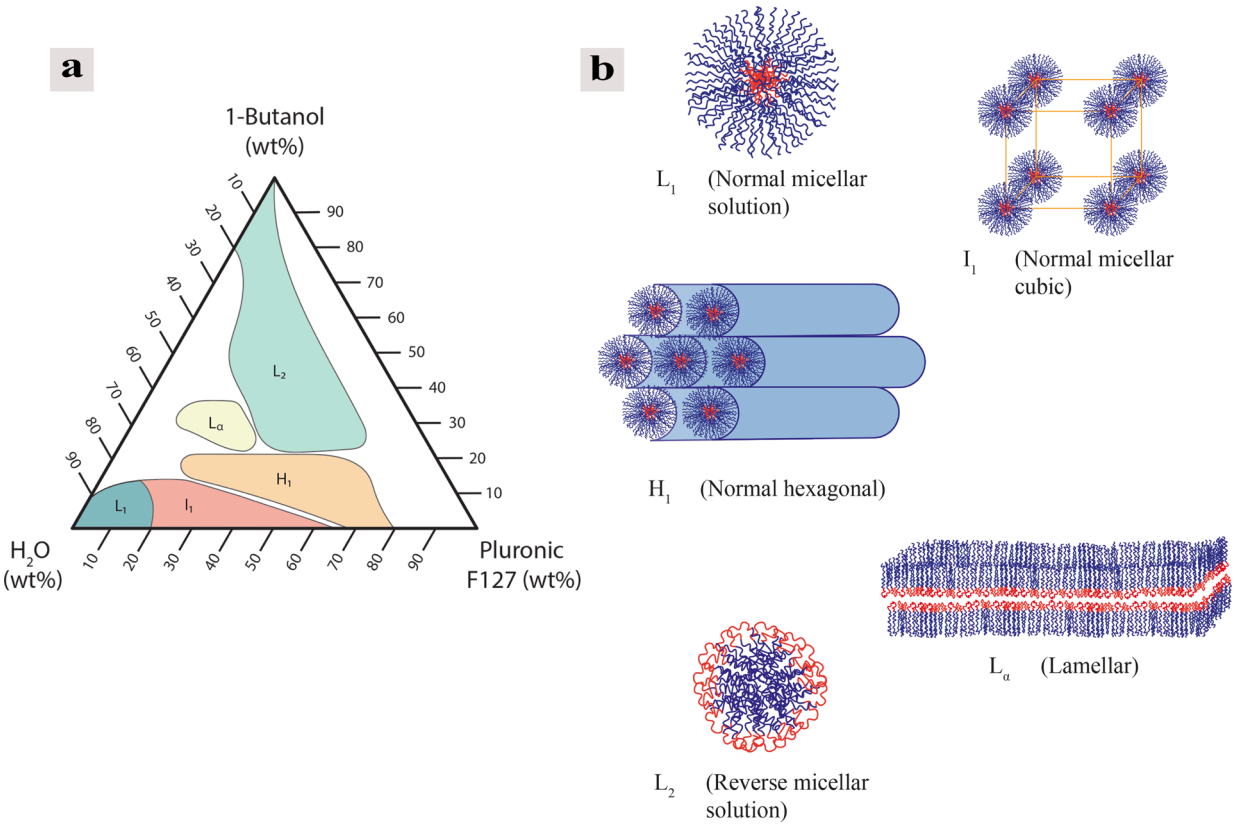

Figure 3. (a) Phase diagram of water, Pluronic F127 and 1-Butanol. L_1 stand for micellar solution, I_1 stand for normal micellar cubic phase, L_α stand for lamellar phase, L_2 stand for reverse micellar solution and H_1 stand for normal hexagonal phase. The figure is adapted from [1]. (b) Illustrations of the LLC phases of (a).

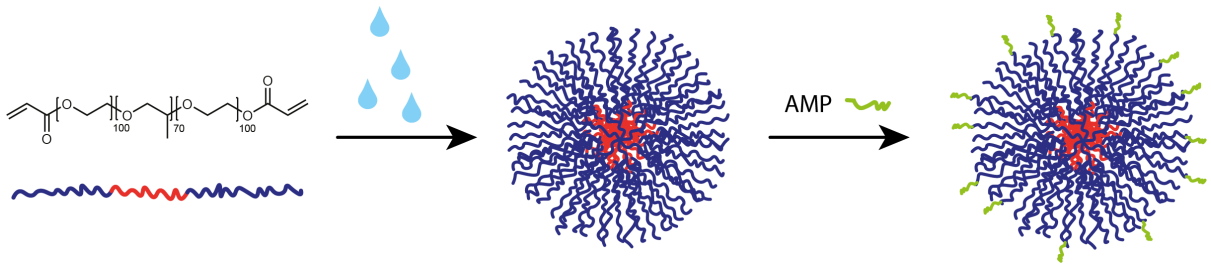

Figure 4. Illustration of micellar formation by Pluronic F-127 that is cross-linked into place, with the consecutive AMP modification of the carboxylic acid groups at the end of the Pluronic molecules. The hydrophobic section is represented as the red core of the micelles, the hydrophilic section is represented as the blue shell, and the AMP is represented as the green segments.

3. Experimental

In the following section, the methods and techniques used in the thesis are shortly described in terms of why and how they were used. For more exact information regarding the procedure, please check the experimental sections of Paper 1 and Paper 2.

3.1. Producing the materials

The Pluronic F127 diacrylate was mixed with water and photoinitiator at concentrations that corresponds to the micellar cubic phase of the phase diagram, denoted as I_1 in Figure 3. For the hydrogel sheets used in Paper 1, the formed gels were spread between two glass slides and stored sealed away overnight in order for the polymers to set into the micellar cubic phase. For the production of particles in Paper 2, the mixed gels were placed at 4°C for at least 2 days before being placed between glass slides. The gels were then cross-linked into solid hydrogels by exposure to UV radiation (λ=302 nm). The hydrogels were then washed for at least two days and could then be modified by covalently attaching AMPs by EDC/NHS coupling.

In order to make the particles that Paper 2 is based on, the cross-linked hydrogels were first washed in water to remove non-cross-linked polymer and initiator. Then they were blended into fragments and then reduced further in size by using an ultra-turrax and sonication. The obtained mixture could then be separated into size by filtration and modified with AMPs by EDC/NHS coupling. The particles could then also be freeze-dried in order to get a fine powder devoid of water that could be stored for longer times and re-swollen rapidly if necessary.

3.2. Material characterization

In order to analyze the water content and swelling potential, the produced materials of both Paper 1 and 2 were put through several cycles of swelling and drying with weigh in after each step. The effectiveness of the peptide modification was evaluated by UV-vis measurements. This was possible due to the presence of tryptophan in the peptide, which has a distinct absorbance at 280 nm. For both sheets and particles the peptide concentration in the surrounding liquid after modification was measured and compared to the stock solution. This gives the amount of peptides that may have covalently conjugated with the hydrogels during post modification of the materials.

To acquire information about the chemical composition of the materials developed in Paper 2, Fourier transform infra-red spectroscopy (FTIR) and Raman spectroscopy were used. The purpose of using these methods was to gain more knowledge about the differences in between sample types and to verify the covalent attachment of the peptides. FTIR measures the molecular vibrations of a material that is exposed to infra-red light. This gives a spectrum from which the molecular composition can be found since molecules vibrate at specific energy levels

due to absorption of light in the infra-red region, resulting in molecular specific peaks. Raman spectroscopy works similarly by aiming a laser at the sample and measuring the molecular specific Raman scattering, resulting in a spectrum with a molecular fingerprint of the sample. Both Raman and FTIR were used since different bonds appear stronger in one of the techniques compared to the other. In this way the two techniques complement each other which could help paint a clearer picture on the nature of the peptide hydrogel interaction.

In Paper 2, small-angle X-ray scattering (SAXS) was used to obtain nano structural information of the self-assembled LLCs formed by the Pluronic F127 polymer. Materials with an ordered structure, when irradiated with X-rays, will scatter the same in a specific scattering pattern which can be picked up by a detector. This makes it possible to detect repeating structures in the material such as cubic ordered micellar structures or hexagonally ordered micellar fibrils. By analyzing the obtained spectrum and comparing it to known LLC structures, it is possible to determine the phase of the lyotropic liquid crystals in the sample. The purpose of using SAXS was to investigate whether the structure was maintained throughout the processing of the LLCs, both in its macroscopic sheet form and particle form.

In order to analyze the size distribution of the particles developed in Paper 2, dynamic light scattering (DLS) was used. By measuring the duration and intensity of the scattering of a laser aimed at a solution, the size and amount of particles in the solution can be determined by using the fact that the particles in the solutions are undergoing Brownian motion. From this, it is possible to get information on the size distribution of the particles, and consecutive runs can even give some information regarding the behavior of the particles, in terms of stability.

3.3. Antibacterial efficacy

The antibacterial effect was evaluated against the following bacterial strains: *Staphylococcus aureus, Staphylococcus epidermidis, Escherichia coli, Pseudomonas aeruginosa,* Methicillin resistant *S. aureus* (MRSA), and multidrug-resistant *E. coli* (MDR-*E.coli*).

For the sheets developed in Paper 1, the antibacterial effect was evaluated by culturing the sheets together with bacteria in tryptic soy broth (TSB) for 24 hours. The samples were then washed with phosphate buffered saline (PBS) and the top surface was then stained with LIVE/DEAD staining. This stain contains two components; SYTO-9 which is membrane permeable and can therefore enter all cells in which it attaches to genetic material and can here be fluorescently activated to emit green light. The other component is propidium iodine which is not membrane permeable and can therefore only enter dead cells with a compromised membrane. When inside the cell it will also attach to genetic material and can be fluorescently activated to emit a red light. With this staining it is therefore possible to get an observable difference between alive and dead cells with the help of a fluorescence microscope. The obtained images can with software analysis give a number on the proportion of dead and alive bacteria on a surface. When compared to non-modified hydrogel sheets, the effectiveness of the peptides can then be determined.

The antimicrobial effect of the particles (Paper 2) was evaluated in two different ways; by minimum inhibitory concentration (MIC) tests and by an agar plate model. In the MIC test, solutions can be tested and, in this case, pure AMP and particles were tried. The solutions were serial diluted by a factor of two in a well plate, and a known concentration of bacteria was added to each well followed by incubation overnight. In the dilution in which no growth was visible the following day is the lowest concentration that is necessary to inhibit the growth of the bacteria and is called the minimum inhibition concentration. This is a clear and rather fast method to determine the effectiveness of an antimicrobial agent. The agar plate model was performed by making slurries of the particles in PBS which were then spread on agar plates where bacteria has been spread just prior. The agar plates were then incubated overnight, and the following day sections in the middle of the spread were obtained with the use of biopsy punches. The sections were then placed in PBS and thoroughly mixed followed by serial dilutions which were placed on agar plates and incubated overnight. The following morning the colonies formed were counted and the original bacterial concentration was calculated. When compared to the non-modified control particles, the antibacterial effect by the addition of AMPs could be evaluated.

To evaluate the covalent attachment of the peptide by the EDC/NHS coupling, a zone of inhibition study was performed (Paper 1). Hydrogel discs were modified either with EDC/NHS activation followed by AMP modification or by just placing them in the peptide solution in an attempt to physically load the LLCs with peptides. Just as in the agar plate model, bacteria were spread on to an agar plate and the disc were then placed on top and the plates were incubated overnight. The following morning, images were taken of the plates to evaluate any potential zone of inhibition around the hydrogel discs, which would indicate that there was a release of peptides occurring from the hydrogels.

In order to gain knowledge regarding the mechanism of action of the particles against bacteria, cryogenic transmission electron microscopy (cryo-EM) studies were performed in Paper 2. Syringe-filtrated particles (<0.22 μm) were AMP-modified and incubated with *S. aureus* for 1 hour. The solution was then plunge frozen in liquid ethane to preserve any biological interactions and viewed with a transmission electron microscope (TEM) under cryo-conditions.

3.4. Proteolytic stability

The antibacterial stability of the peptides attached to the hydrogel sheets were evaluated by placing AMP-modified hydrogels in serum and then taking them out from the serum at certain time intervals. As described in Paper 1. The hydrogel sheets were then washed and placed in well plates and incubated together with *S. aureus* for 24 hours and were then stained with LIVE/DEAD staining and imaged with fluorescence microscopy. The proportion of dead cells were then plotted against time and when compared to the non-modified control hydrogels the stability of the antimicrobial effect could be evaluated.

3.5. Cytotoxicity

In order to make sure that no adverse effects of the manufactured materials of Paper 1 were seen, in terms of being harmful to mammalian cells, cytotoxicity studies were implemented. More specifically, a method called MTT-assay was performed. For this, the hydrogels were placed in cell media at 37 °C for 3 days. The hydrogels were then removed by simply taking a tweezer and plucking them out. The sample exposed media was then placed in well plates to which a certain number of cells was added. The cells used was primary human dermal fibroblasts since it is vital that these cells are not affected for a potential wound care application. The cells were left to grow for 3 days in the sample exposed media, along with controls. After 3 days the media was changed and MTT was added to the wells. Alive and healthy cells will break down the MTT to soluble Formazan which also can be measured by spectroscopy. The cells were therefore lysed after 4 hours of cultivation and the absorbance was read by a microplate reader. After comparing to a negative control (cells grown in just pure media) the cytotoxicity of the material could be evaluated.

3.6. Pilot *in vivo* study

In Paper 1, a pilot *in vivo* study (approved by the Local Ethical Committee for Laboratory Animals) was performed where the hydrogels were placed in pockets surgically cut on to the back of seven female Sprague-Dawley rats. Each rat had six pockets with control hydrogels in three pockets and AMP-modified hydrogels in the other three. One set of hydrogels were left without bacteria and to one set 50 µl of *S. aureus* of a concentration of 10^4 CFU/ml were added and to the last set 50 µl of *S. aureus* of a concentration of $2*10^6$ CFU/ml were added. Animals were sacrificed after 24 or 72 hours and the exudate around the hydrogels were gathered as well as the hydrogels themselves. The CFU count of the extract and the hydrogels were then evaluated.

4. Result and discussion

4.1. Material preparations

A general scheme of the production process of both the hydrogel sheets and the particles is presented in Figure 5. In Figure 5a, it is shown that the mixed components first formed a very foamy gel. The same gel after it has been stored at 4 °C over a weekend can be seen in Figure 5b and c. Depending on the temperature of the gel at this stage, it will change from being a liquid at 4 °C to being a gel at room temperature. This behavior can be utilized to ease casting or even 3D-printing to form the gels into desired shapes. Since the gel then can be cross-linked solid, as seen in Figure 5d, the desired final shade of the material is easy to manipulate. The hydrogel sheets and discs studied in Paper 1 was however not made exactly like Figure 5d. Instead, the foamy gel of Figure 5a was centrifuged and placed between glass slides where it was left for a day sealed away from light and then cross-linked. This resulted in a bit more air bubbles but otherwise similar appearance. The particles used in Paper 2 were made using the cross-linked hydrogels as the starting material. After the hydrogels had been washed for a few days they were grinded up, reduced further in size using an ultra-turrax and sonicated to form the slurry seen in Figure 5e. For some experiments it was necessary to have the particles completely dry. The particles were then freeze-dried to maintain the structure as much as possible. The results from this can be seen in Figure 5f.

Both the hydrogel sheets and the particles were hydrophilic and absorbed water into their structures. Roughly 90% of the weight is water in fully swollen state. From the UV-vis studies we do, however, know that the AMP modification was rather different for the two systems. The hydrogel sheets, when modified as 1 mm thick discs, took up 1 mg of AMP per gram of swollen hydrogel. The particles, on the other hand, took up 3.3 mg of AMP per gram of swollen particles. This strongly indicates that the available surface is a greater driving force for the modification compared to the available mass/volume.

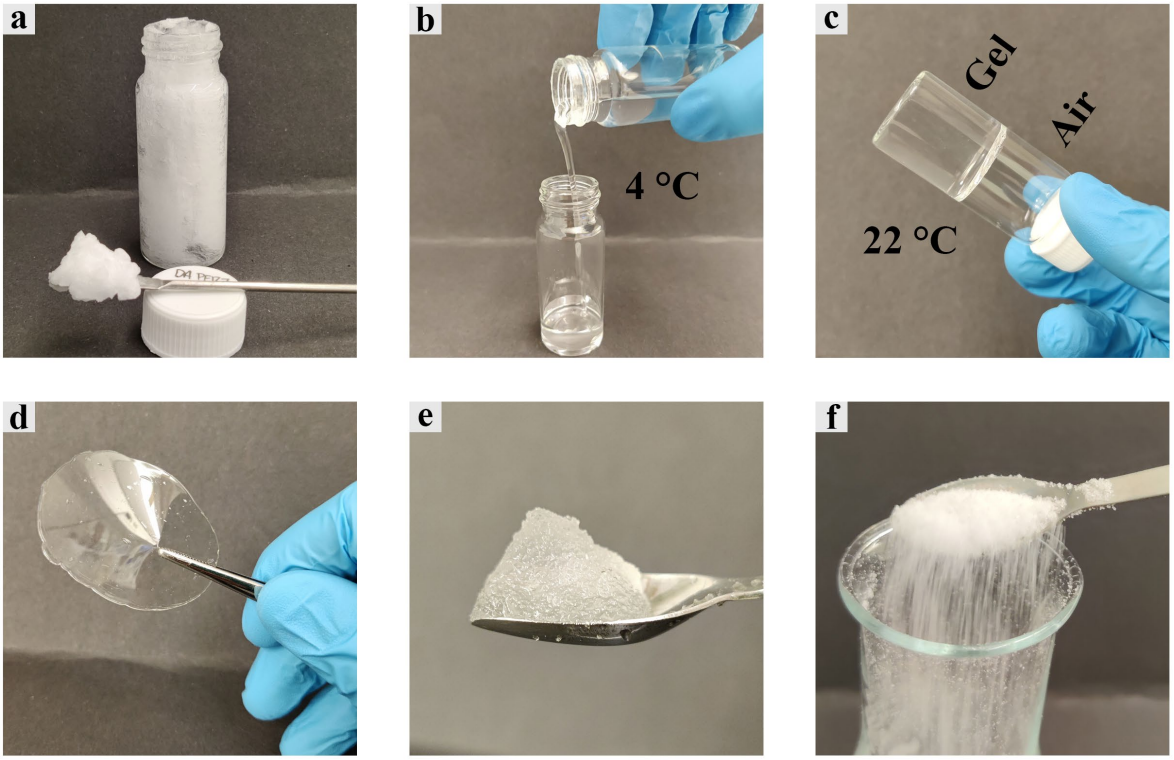

Figure 5. Images taken of the different steps of the particle formation process. (a) The gel mixture directly after mixing. (b) The gel solution at 4 ℃ after being stored in the fridge for 72 h. (c) The same solution after it has equilibrated to room temperature. d) The hydrogel after it has been cross-linked between two glass slides. (e) The particles made from the hydrogels by grinding, using an ultra-turrax and sonicating. (f) The particles after they have been AMP-modified and freeze-dried.

4.2. Material characterization

4.2.1. Chemical characterization

Figure 6 shows the FTIR results of pure AMP powder, freeze-dried control particles, freeze-dried AMP-modified particles, and the DA-PF127 powder. Figure 6a shows the full spectra of the four samples. The main thing one can tell here is that the Pluronic F-127 fingerprint between 500-1500 cm^{-1} was maintained for all the Pluronic containing samples, indicating that no major changes were made to the structure. In Figure 6b, the spectra have been zoomed in on 1520-1820 cm^{-1} to closer illustrate changes in the ketone area. Between the DA-PF127 sample and the freeze-dried control particles there was a slight peak shift and broadening of the peak at 1725 cm^{-1} in the DA-PF127 sample to 1735 cm^{-1} in the control particles sample. In the DA-PF127 sample we have a conjugated ester bond and the two most likely scenarios for the type of ketone in the control particles are a non-conjugated ester or a carboxylic acid group. Both of these bonds are expected to give rise to absorbance at higher wavenumbers. It is therefore very difficult to claim what type is contributing to the observed change strictly from the data. However, we know that the hydrogel is in fact solid-like, which can only be achieved if the

majority of the ketone groups are in an ester bond. It is therefore speculated that only a minority of the ketones are found as carboxylic acids. The peak location does not shift significantly for the AMP-modified particles, further strengthening this speculation. There is however a slight difference in peak appearance, as the peak at 1735 cm^{-1} for the AMP-modified particle is not as deep and have a rounder appearance. This could be due to the fact that the carboxylic acids in the mixture forms peptide bonds through EDC/NHS activation. The amides of the peptide bonds in the peptide itself are giving rise to the broader peak at ~1660 cm^{-1} found in both AMP containing systems. As the freeze-dried AMP-modified particles are completely void of water it is safe to say that the found AMPs are incorporated into the LLCs. It is however more difficult to claim anything regarding the covalent attachment from this data, especially since potential peptide bonds formed by the carboxylic acid groups would be engulfed by the amide contribution of the peptide itself.

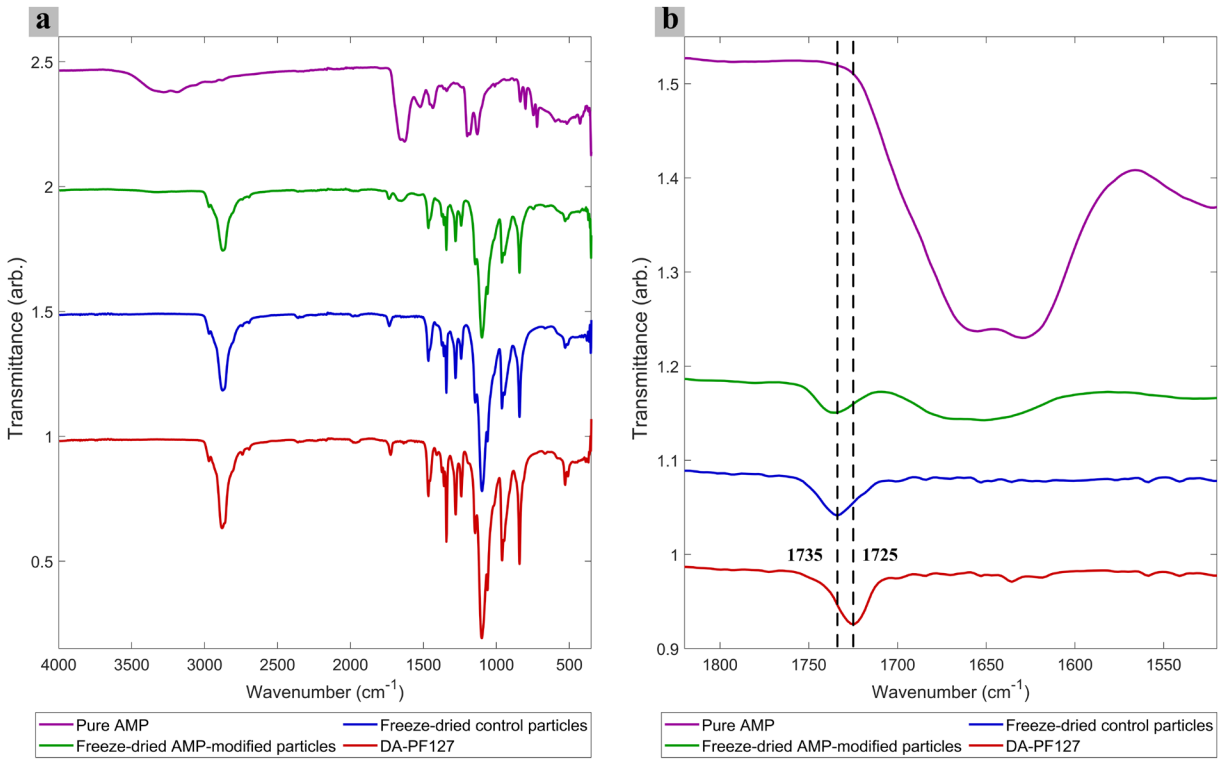

Figure 6. FTIR results of pure AMP (purple), freeze-dried AMP-modified particles (green), freeze-dried control particles (blue) and the DA-PF127 (red). (a) The full spectra. (b) A zoomed in section of wavenumbers between 1520-1820 cm^{-1}. Two lines have been drawn in b) where the left one is drawn at 1735 cm^{-1} and the right one is drawn at 1725 cm^{-1}.

These observations are further supported by the results from the Raman spectroscopy, seen in Figure 7. Powder from the same samples were examined, and the main peaks that change in between the samples are marked with arrows in the figure. Between the DA-PF127 sample and the control particles there were two peaks at ~1640 cm^{-1} and ~1730 cm^{-1} that disappeared. These peaks correspond to C=C bonds, which fits well with the vinyl group of the acrylate.

Their disappearance marks that this is how the system is cross-linked together. Between the control and the AMP-modified samples there are three small new peaks at ~750 cm^{-1}, ~1010 cm^{-1}, and ~1550 cm^{-1} that appear in the AMP-modified sample. All of these peaks are also found as narrow strong peaks of the pure AMP sample, further indicating the incorporation of AMP into the material. The peak at 1010 cm^{-1} is most likely due to the guanidino groups of the arginine amino acids and the peak at 1550 cm^{-1} is most likely due to the indole groups of the tryptophan amino acids. That the peaks are so small in the AMP-modified samples, for both FTIR and Raman, is due to the fact that the peptides only contribute to roughly 3.3% of the dry weight of the particles. The spectra are therefore mainly consisting of the contributions from the PF-127 and the interactions between the structure and the peptides was very difficult to determine.

4.2.2. Structural characterization

The results obtained from the SAXS measurements can be seen in Figure 8. The clear diffraction peak at these q-values in all the spectra indicate that an ordered nanostructure, most likely a micellar cubic structure was indeed present in all the samples [1, 69]. Based on prior literature data on the same composition, it is known that DA-PF127 and water forms a micellar cubic structure. Furthermore, it was evident that the same structure was found for the freshly cross-linked hydrogel sheets (30 wt% Pluronic, 70 wt% water) as for both of the freeze-dried particles. This indicates that the LLC was not affected by neither the steps taken in order to make the particle nor that the AMP-modification made an observable difference in the structure. This is not really surprising, since the structure is fully cross-linked before the addition of peptides is made. There was a slight peak shift observed for the fully swollen particles compared to the other spectra. The peak shifted roughly 0.005 $Å^{-1}$ to a higher q-value. This indicates that the spacing has become smaller in between the structure. The explanation for this could be that the micelles of the LLCs has swollen by taking up water, but since the structures are cross-linked together the structures cannot move too much away from each other, effectively making the distance between them smaller.

A number of reasons may contribute to the low SAXS signal and thereby the absence of secondary peaks obtained from the materials namely low sensitivity of the SAXS instrument and in-situ drying of the materials during measurements leading to higher probability of random scattering. It is therefore not possible to draw any conclusions regarding the structure solely from the plots. However, the phases of Pluronic F-127 have been thoroughly studied, and the concentration used to make the gels has been determined to be in the micellar cubic phase. Since the peaks did not change in appearance it can be deducted that this phase is maintained throughout the process. This means that both the sheets and particles are made up of self-assembled Pluronic F-127 in micellar cubic LLCs. This is further supported by earlier work by our group which have look in to similar composition of the DA-PF127 and showed that the micellar cubic structure was present in the gel formed by 35 wt% DA-PF127 and 65 wt% water, and preserved after cross-linking [70].

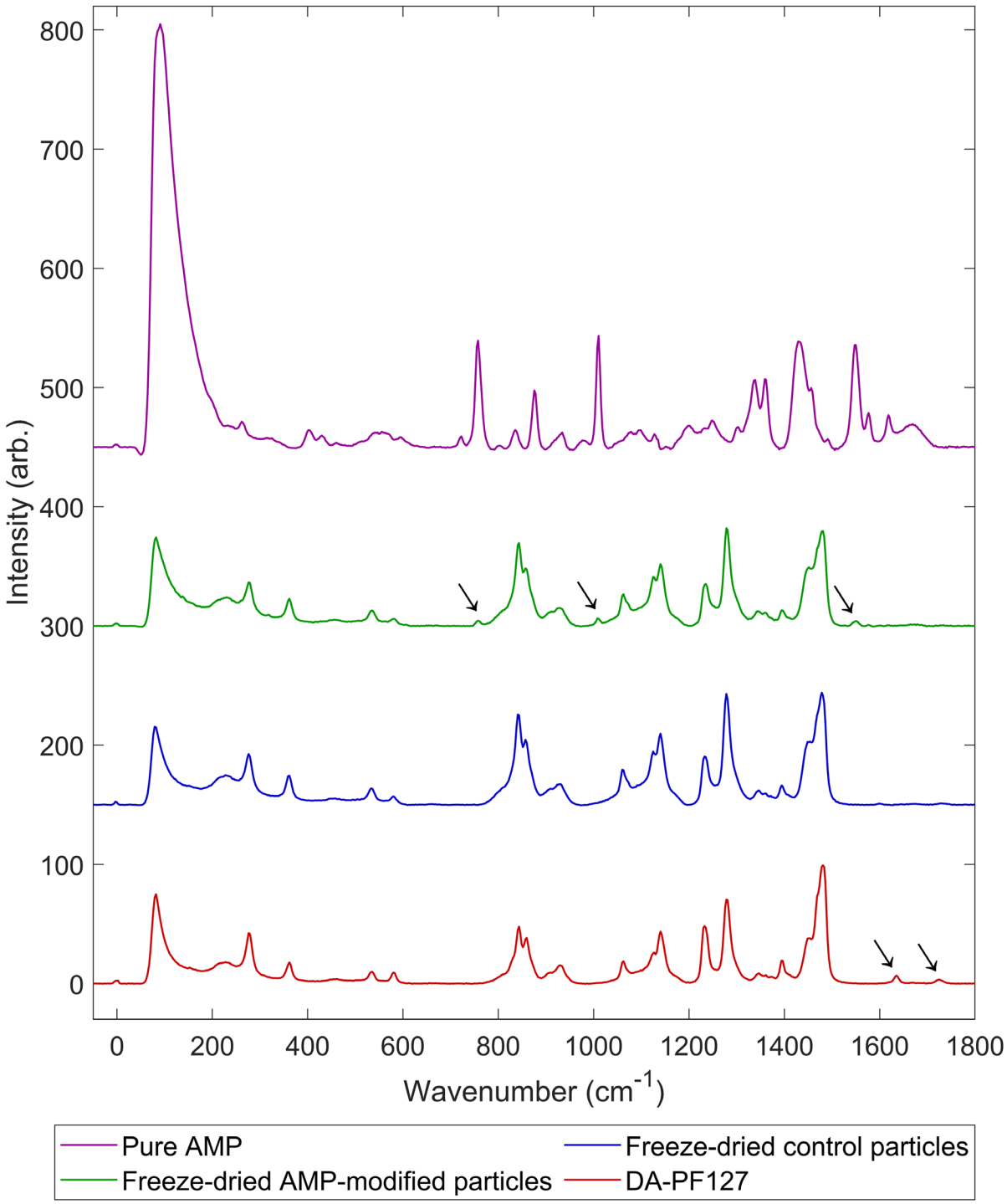

Figure 7. The measured Raman spectra for the pure AMP (purple), freeze-dried AMP-modified particles (green), freeze-dried control particles (blue), and DA-PF127 (red). The black arrows indicate the peaks that are changing in between samples.

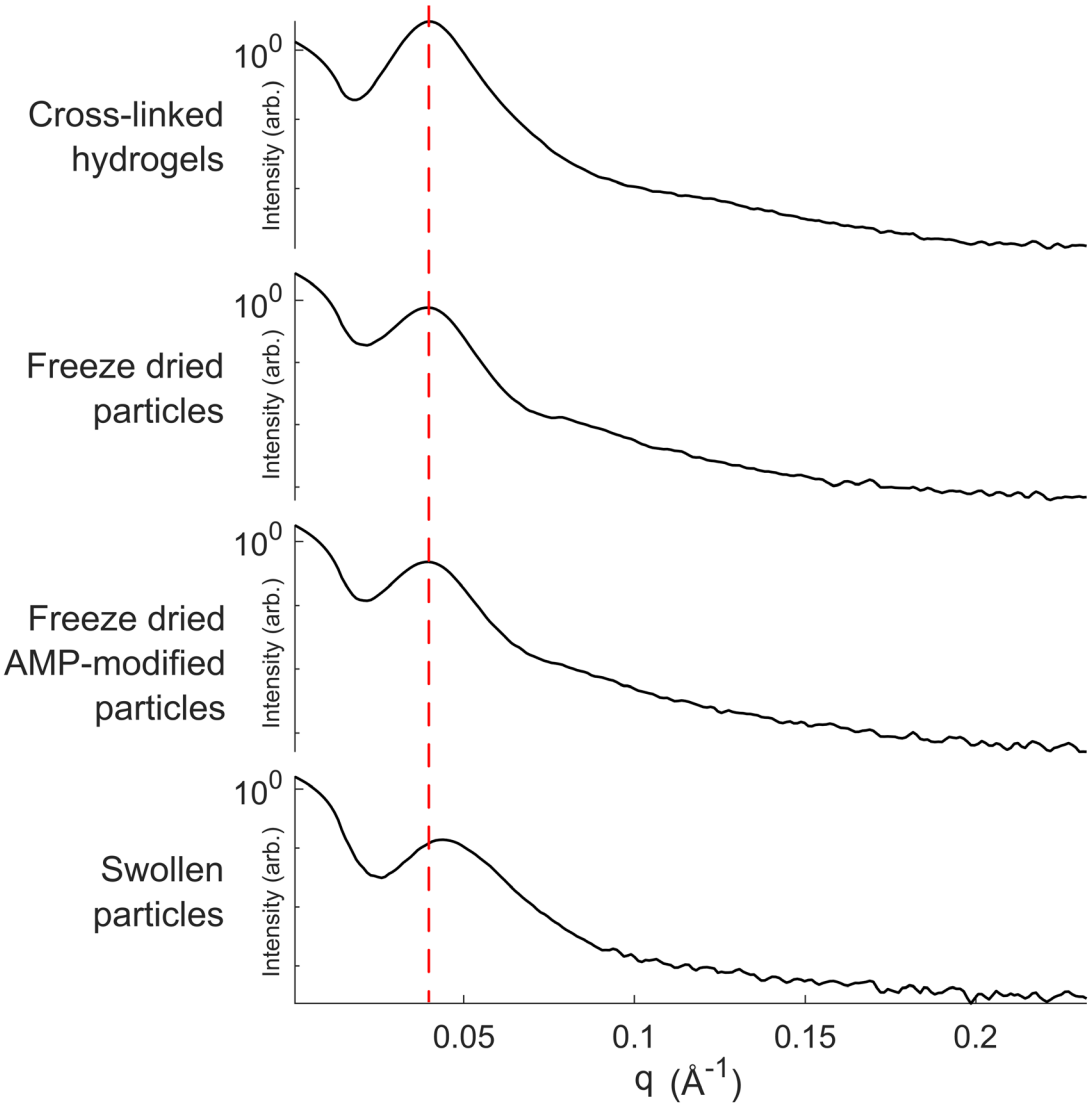

Figure 8. The SAXS diffractograms for the cross-linked hydrogels (30 wt% DA-PF127, 70 wt% water), freeze-dried control particles, freeze-dried AMP-modified particles, and fully swollen control particles. All samples were measured in between tape, which has been removed as a background from the other samples.

The size distribution of the particles developed in Paper 2 is presented in Figure 9 and Figure 10. The size distribution of the whole set of particles straight after they were made can be seen in Figure 9. It is evident that a very broad distribution was obtained. Depending on whether a volume-based distribution or a number-based distribution was used, the appearance changed significantly. What this means is that the vast majority of the mass can be found in particles with a size between 100-500 µm, while the majority of the particles have a size between 2-30 mm. This means that if a particle was chosen randomly it is more likely to be a particle with this size.

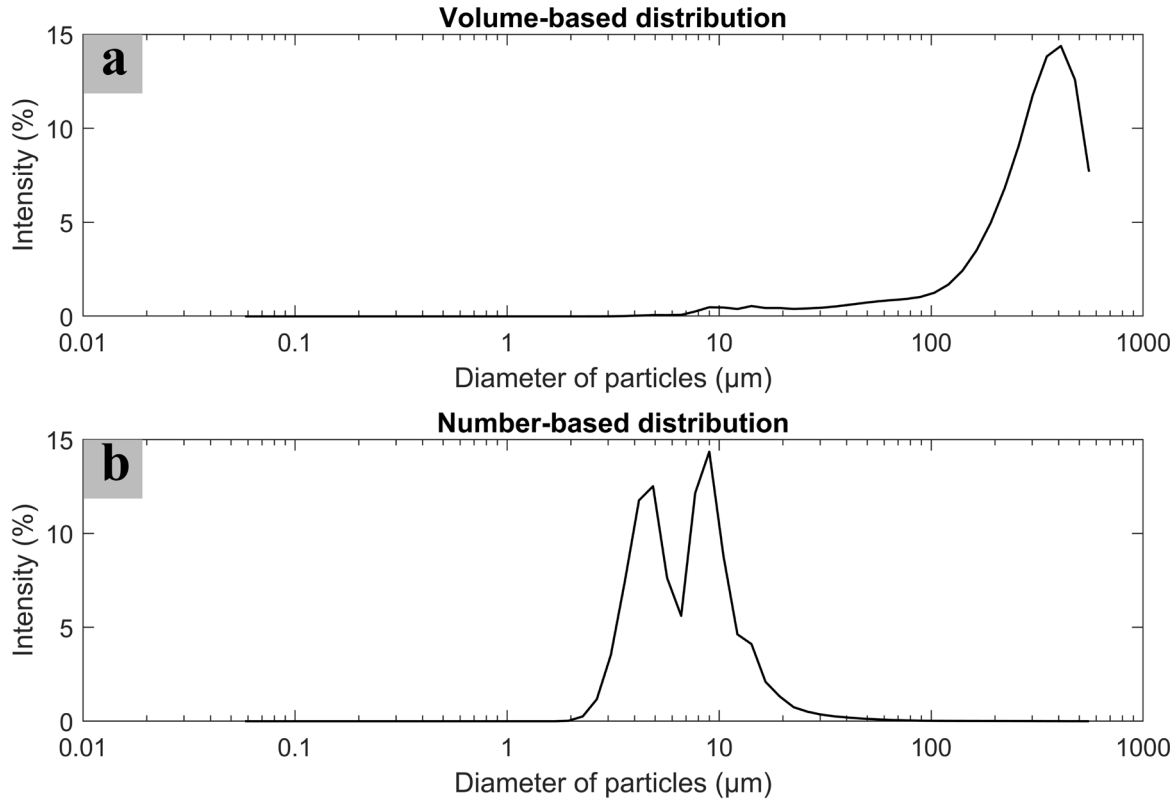

Figure 9. Size distribution of the whole range of control particles. (a) The volume-based distribution. (b) The number-based distribution.

The size distribution of a subset of particles that have gone through a 6 μm filter is presented in Figure 10, where control particles are presented in Figure 10a and AMP-modified particles are presented in Figure 10b. The data of the control particles showed two clearly distinct distributions, between 20-60 nm and 90-350 nm. The three consecutive runs showed very similar results indicating that the particles at least were stable for these shorter periods of time. The data for the AMP-modified particles, however, showed a less clear distribution. The distribution of the three consecutive runs were a bit different in between measurements, with a broader span (20-700 nm) compared to the control particles. This indicates that the AMP-modified particles are not stable even for the short time of the experiment. The explanation to this change of distribution is speculated to be due to the properties of the AMPs themselves. The tryptophan end-tag is very hydrophobic which could cause the particles to become 'sticky'. This means that the hydrophobic effect might cause the tryptophan groups of the peptides attached to different particles to aggregate, causing the observed shift to bigger sizes. The arginine groups of the peptides, on the other hand, should work as repulsive forces, due to their positive charges, acting against aggregation. This could be the reason why the second run has a distribution more like that of the control particles and why run 1 and 3 have a broader distribution. Further experiments are however necessary to study the interaction.

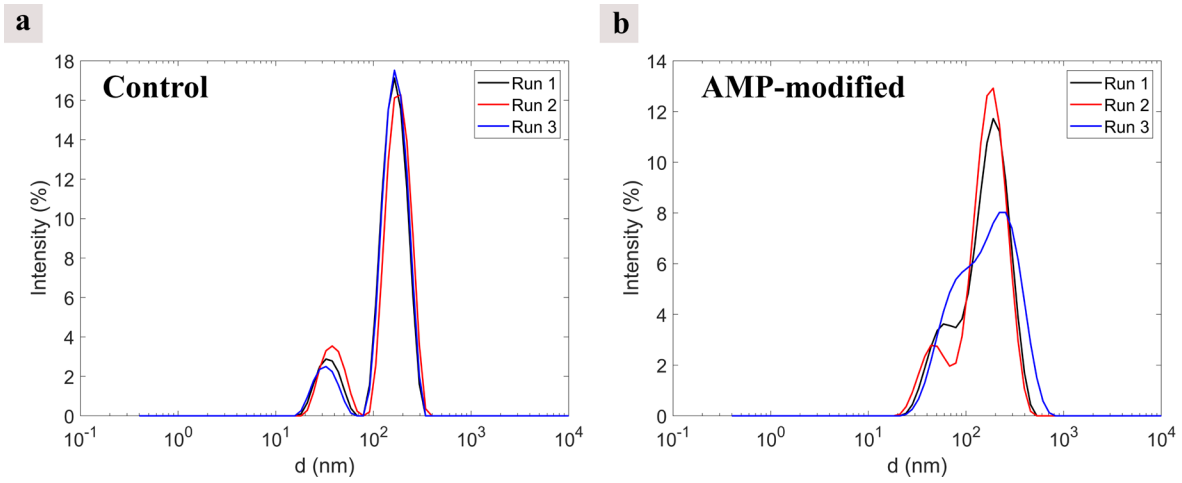

Figure 10. Size distributions (intensity-based) measured by DLS of the filtrated (<6 µm) particles. (a) The size distribution of non-modified control particles over three consecutive 60 second runs. (b) The size distribution of the AMP-modified particles over three consecutive 60 second runs.

4.3. Antimicrobial efficacy

Images of the surfaces of control and AMP-modified hydrogel discs developed in Paper 1 after 24 hours of incubation with *S. aureus, S. epidermidis* and *P. aeruginosa* are presented in Figure 11. It was clear that the number of alive cells (stained green) was found in much higher quantities on the control samples compared to the AMP-modified samples. On the contrary, the number of dead cells (stained red) was much higher on the AMP-modified samples compared to the respective control samples. The reduction of alive cells strongly indicates that biofilm formation on top of the hydrogels was effectively prevented by binding AMPs to the hydrogels. The increase of dead cells strongly indicate that the biofilm prevention was due to the bacteria being killed. The most likely mechanism of action is contact killing, which also explains why there are some alive bacteria found on the AMP-modified samples. When the hydrogel samples are put in a solution there will always be a deposition of new bacteria to the surface. At some point this will result in the surface being saturated and therefore not being able to kill the new bacteria. Noticeable is that the gram-negative bacteria *P. aeruginosa* did not appear to cultivate the control hydrogel surfaces (Figure 11c) in the same extent as the two other bacteria strains did (Figure 11a and b). Since all of these bacteria are commonly found in infected wounds on humans, antibacterial activity against them is of high relevance with the application in mind.

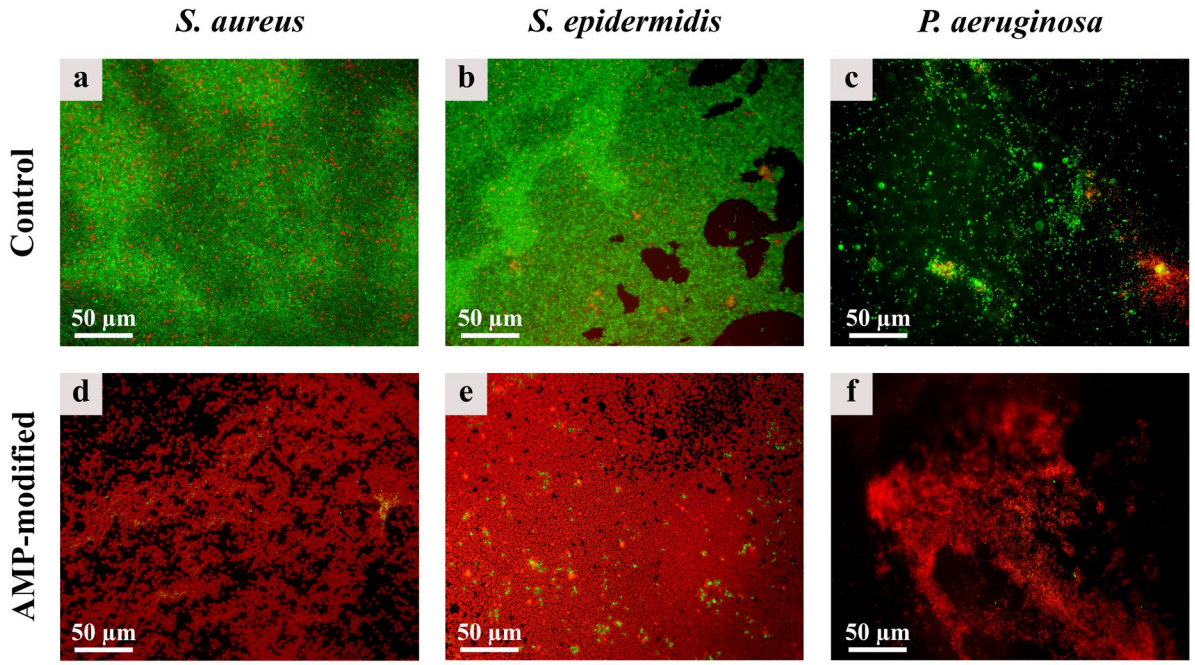

Figure 11. Images of bacteria on top of hydrogels that has been cultivated for 24 hours and where the alive cells have been stained green by SYTO 9 and the dead cells has been stained red by Propidium iodine. (a) S. aureus on top of a control hydrogel. (b) S. epidermidis on top of a control hydrogel. (c) P. aeruginosa on top of a control hydrogel. (d) S. aureus on top of an AMP-modified hydrogel. (e) S. epidermidis on top of an AMP-modified hydrogel. (f) P. aeruginosa on top of an AMP-modified hydrogel. All scalebars in the images are 50 µm.

In an attempt to easily get an overview of the potential antibacterial effect, a macro in the software Fiji was used to calculate the fraction of the surface that was green (alive cells) and the fraction that was red (dead cells). The macro was not perfect but with enough images it painted a clear picture. The graphs for the calculated values for the study against *S. aureus, S. epidermidis* and *P. aeruginosa* can be seen in Figure 12. The results show more of the same, where the amount of alive cells was lower for all bacteria on top of the AMP-modified samples compared to the control samples. Furthermore, the amount of dead cells was also greater for the AMP-modified samples compared to the control samples.

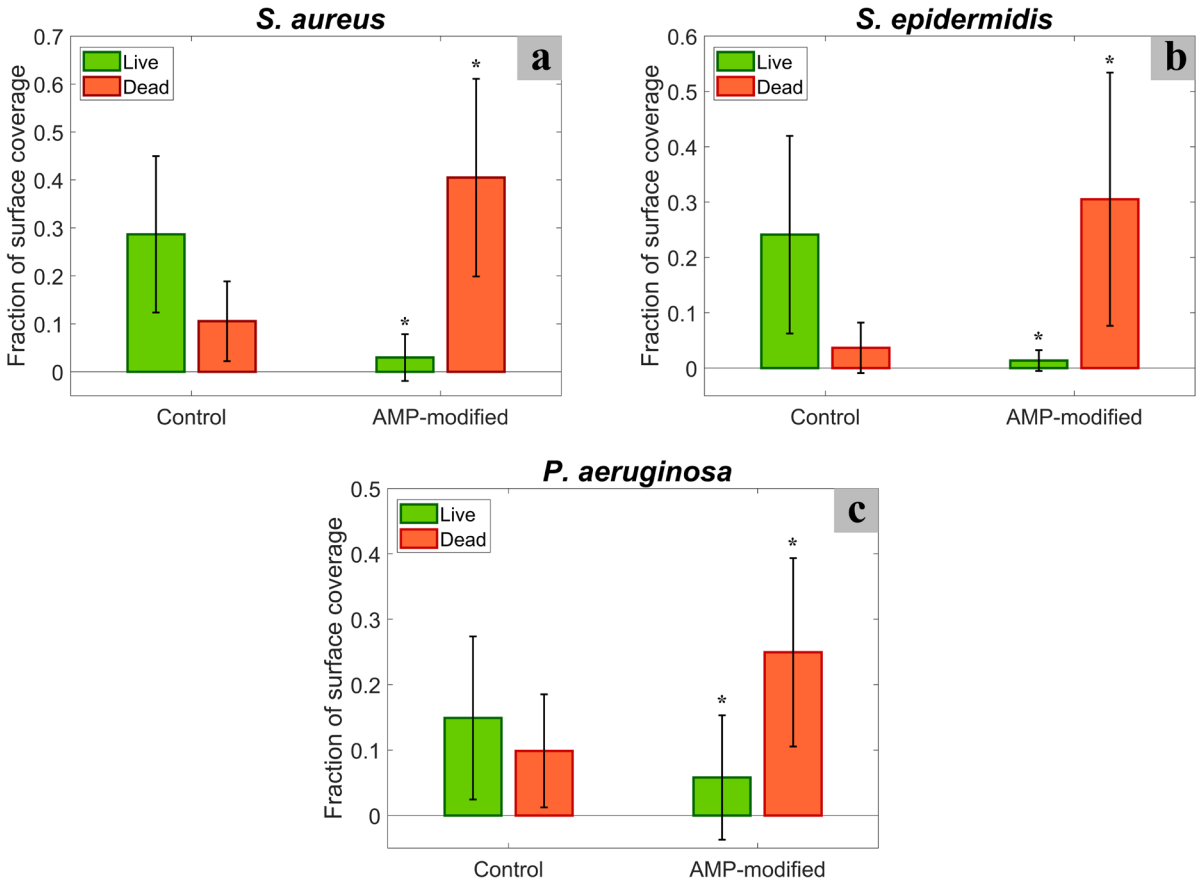

*Figure 12. Quantitative analysis of the surface coverage of alive and dead cells of S. aureus (a), S. epidermidis (b), and P. aeruginosa (c) on top of control and AMP-modified hydrogels. The values were obtained by analyzing the fluorescent images from n=9 samples using Fiji software. * indicates a statistically significant difference compared to the corresponding control with p<0.05, and the error bars show the standard deviation.*

The same test was also done against two antibiotic resistant bacterial strains. The results from these tests can be seen in Figure 13 and Figure 14. For the MRSA it was clear that it had a good effect, and the results did not differ much from that of non-resistant *S. aureus*. The amount of alive bacteria significantly decreased on the surface and the amount of dead bacteria significantly increased. For the MDR-*E. coli* the results were similar to the other gram negative bacteria tested. There were not a lot of attached bacteria to the control surface and it was therefore not much less alive bacteria found on the AMP-modified surface. It was, however, significantly more dead bacteria found on the AMP-modified surface for this strain, strongly indicating that the AMP-modified surface was fully capable of killing the resistant bacteria.

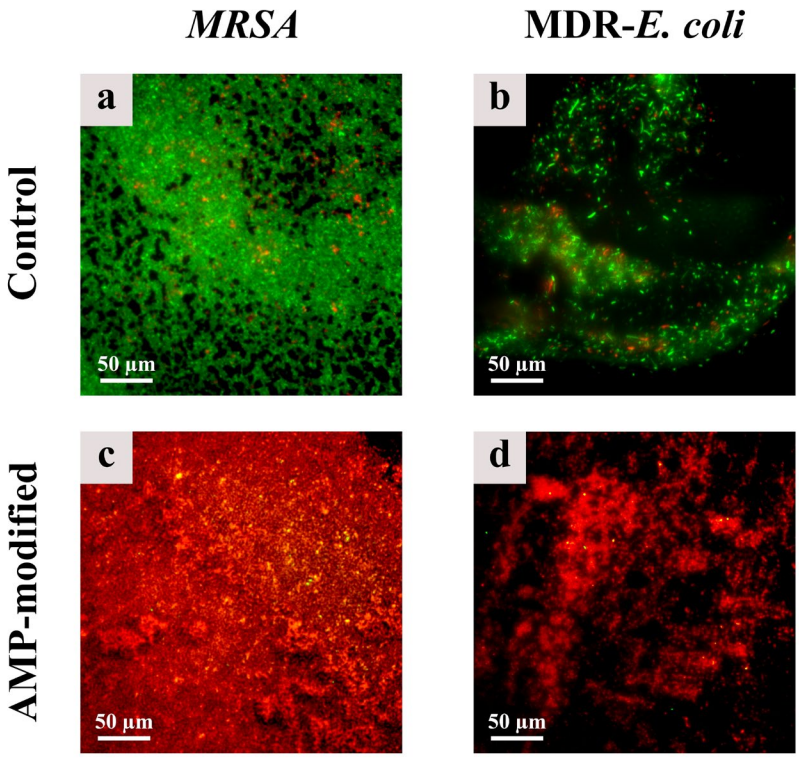

Figure 13. Images of bacteria on top of hydrogels that has been cultivated for 24 hours and where the alive cells have been stained green by SYTO 9 and the dead cells has been stained red by Propidium iodine. (a) MRSA on top of a control hydrogel. (b) MDR-E. coli on top of a control hydrogel. (c) MRSA on top of an AMP-modified hydrogel. (d) MDR-E. coli on top of an AMP-modified hydrogel. The scale bars in all images are 50 µm.

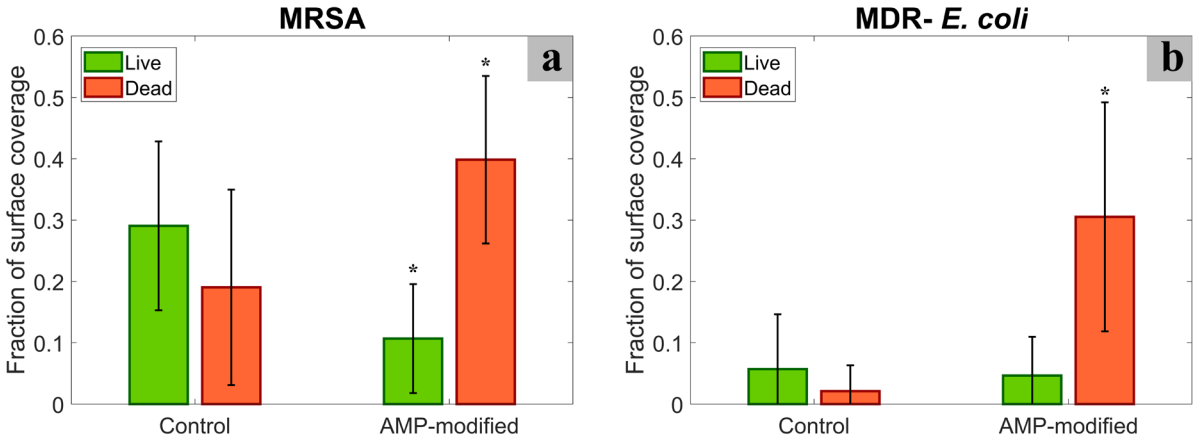

*Figure 14. Quantitative analysis of the surface overage of alive and dead cells of (a) MRSA and (b) MDR-E. coli on top of control and AMP-modified hydrogels. The values were obtained by analyzing the fluorescent images from n=9 samples using Fiji software. * indicates a statistically significant difference compared to the corresponding control with $p<0.05$, and the error bars show the standard deviation.*

The antimicrobial activity of the pure AMP and the AMP-modified particles (Paper 2) in solution against *S. aureus, S. epidermidis* and *P. aeruginosa* is presented in Table 1. The pure AMP showed a very low MIC for both *S. aureus* and *E. coli* but unsurprisingly a bit higher concentration was necessary in order to stop the growth of *P. aeruginosa*. The AMP-modified particles showed a similar trend but when recalculated to the corresponding peptide concentration of the particles it was evident that the activity was a bit lower when bound to the particles. This is not really surprising, as the peptides have lost some degree of freedom in terms of restricted moving. For both *S. aureus* and *E. coli* the concentrations are still relevant, and 30 mg/ml of particles is still clearly a solution. Up towards 250 mg/ml of particles and the solution is starting to become more of a slurry, which is not really suitable for all applications. Important to keep in mind is that the smallest particles (<6 µm) are not present in the solution, which, if present, could have resulted in lower MIC, since they have a better mobility.

Table 1. The measured MIC values against three bacterial strains. N=3 and if different concentrations were seen at different runs, an interval of concentrations is presented.

Name	*S. aureus*	*E. coli*	*P. aeruginosa*
Pure AMP	1.56 µM	1.56 – 3.12 µM	6.25 – 12.5 µM
AMP-modified particles (swollen weight)	7 – 30 mg/ml	14.3 – 31.25 mg/ml	125 – 250 mg/ml
AMP-modified particles recalculated to AMP concentration	12 – 51 µM	24.4 – 53.4 µM	213 – 427 µM

Perhaps a more relevant experiment for wound care applications is the agar plate model from which the results against *S. aureus* are presented in Figure 15. Figure 15a shows an image taken of an agar plate after cultivation with the control spread on the left and the AMP-modified spread on the right. Straight from the appearance it was clear that the bacteria were growing and thriving around the control particles, which was not the case around the AMP-modified particles as the color was much more transparent. This was also clear from the measured CFU count from biopsy punches taken from the middle of the spreads. The results presented in Figure 15b revealed that the AMP-modified particles lowered the bacterial load by log4 compared to the control particles. The control samples had a bacterial load of $2.5 \pm 1.0 * 10^8$ CFU/ml and the AMP-modified samples had a bacterial load of $1.7 \pm 2.5 * 10^4$ CFU/ml. Recalculated to a surface concentration, this corresponds to $1.98 \pm 0.79 * 10^9$ CFU/cm^2 for the control samples and $1.35 \pm 1.98 * 10^5$ CFU/cm^2 for the AMP-modified samples. This potential to greatly reduce the bacteria present in a wound could make wonders, giving the leukocytes

of the inflammatory response a breathing room and only having to deal with stragglers not caught by the particles.

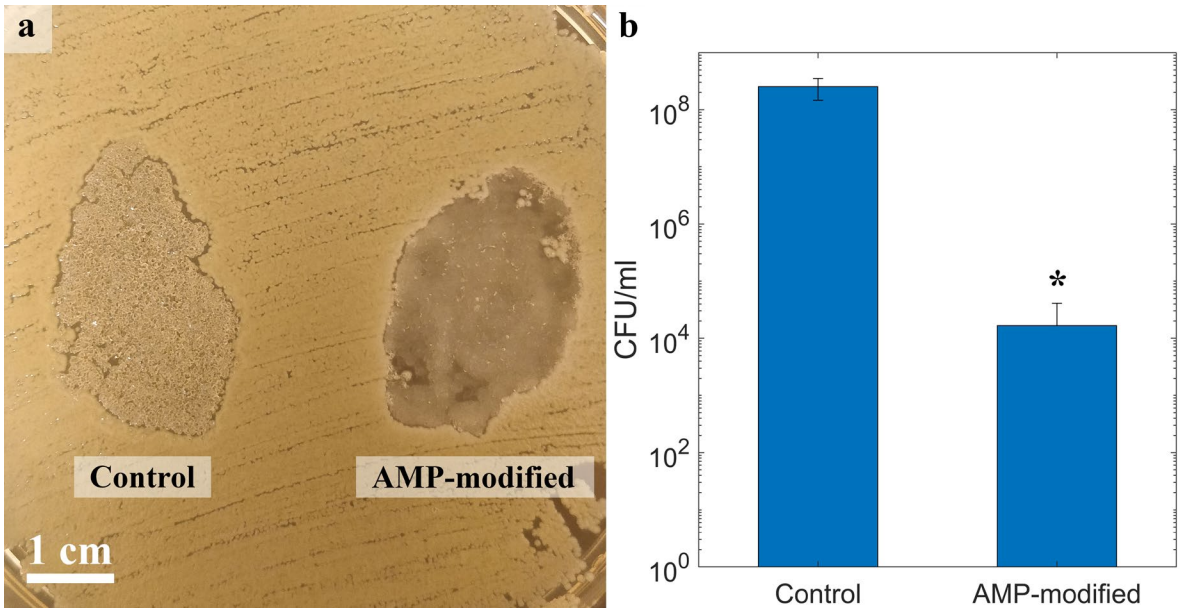

*Figure 15. (a) An image of the top of an agar plate cultivated over night with S. aureus. Control particles are spread on the left and AMP-modified particles are spread on the right. The scale bar is 1 cm. (b) The measured CFU/ml of biopsy punches taken from the middle of the spreads shown in a). n=9 and the error bars show the standard deviation. * indicates a statistically significant difference compared to the control with $p<0.05$.*

To demonstrate the covalent attachment of the AMPs to the hydrogel discs used in Paper 1, a zone of inhibition study was performed, and the result is presented in Figure 16. Hydrogel discs were either left non-modified or activated by EDC/NHS followed by AMP modification, or they were placed in the AMP solution without priorly being activated by EDC/NHS (named here as physically absorbed AMPs). After cultivating overnight on top of an agar plate streaked with *S. aureus* the images in Figure 16 were taken. No clear zone of inhibition was seen around neither the control hydrogels nor the covalently AMP-modified hydrogels. A clear release from the physically absorbed AMPs was, however, evident although it was not the most perfect zone of inhibition (i.e. there are some clear colonies close to the discs and the edge of the zone in not sharp). The covalent attachment reaction is never 100%, but the non-attached peptides that are not washed away of the covalently modified sample are evidently in such a low concentration that they do not show an antibacterial effect. From these results it can therefore be deducted that the majority of the AMPs taken up by the hydrogels activated by EDC/NHS were covalently attached to the LLCs. A similar reasoning can be made for the AMP-modified particles of the agar plate model in Figure 15 as no clear zone indicating release of peptides was present around the AMP-modified particle spread.

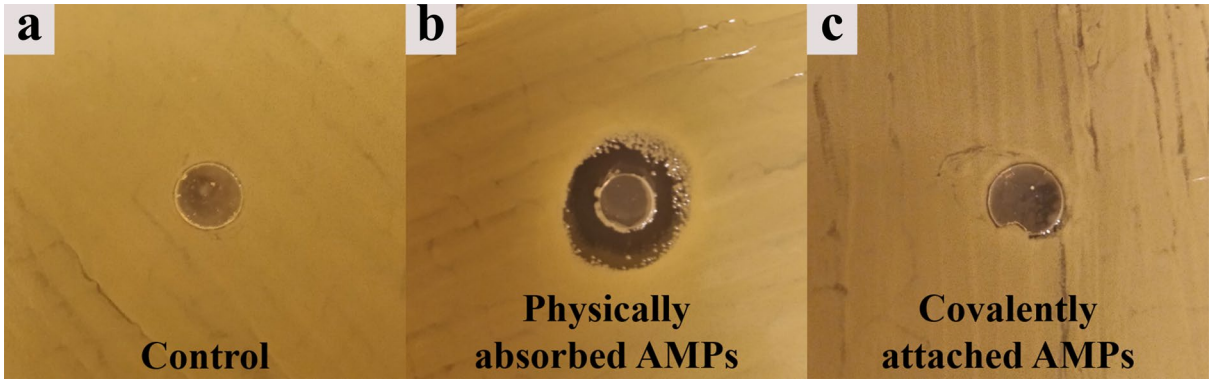

Figure 16. Images taken of (a) control hydrogel, (b) hydrogel with physically loaded AMPs, (c) hydrogel with covalently attached AMPs cultivated overnight on agar plates spread with S. aureus. All hydrogel discs were punched out with a 4 mm Ø biopsy punch, before swelling.

To study the potential interaction between the particles developed in Paper 2 and the bacteria, cryo-EM was implemented. This technique makes it possible to study biological interactions within samples as it is locked in place by plunge-freezing, for example a bacterial solution, in liquid ethane and then keeping it in liquid nitrogen throughout the imaging process. As described earlier, this study aimed at investigating the interactions between the AMP-modified hydrogel particles and the bacteria at the sub micrometer level. The images obtained from the study are presented in Figure 17. From Figure 17b and Figure 17d it is clear that there is an attraction between the particles and the bacterial surface. The particles appear to be deformed close to the bacteria and in Figure 17b the cell wall/membrane of the bacterium closest to the particle even appear to be distorted somewhat (marked with a red arrow in the image). This suggests that the antibacterial mechanism have to do with interactions with the cell wall/membrane of the bacteria. A few limitations of this analysis were however evident, the bacterial strain used (*S. aureus*), given their large size (≈1 μm) presented as thick large spheres thereby minimizing the contrast required for capturing clear transmission electron micrographs. Additionally, as the ice that formed around the cells was quite thick, it gets darker and darker closer to the cells. This is also speculated to be the reason behind the fact that only particles that match the size distribution of bigger particles (~250 nm) were found close to the bacteria. Smaller particles were seen elsewhere in the samples and it is speculated that they are also present closer to the bacteria but does not show up due to the ice. It would be of great interest to study the interaction further using a strain where the cells are a bit smaller, like mini-*E- coli*. It would also be beneficial to have a higher concentration of particles at this size as it was time consuming finding interactions.

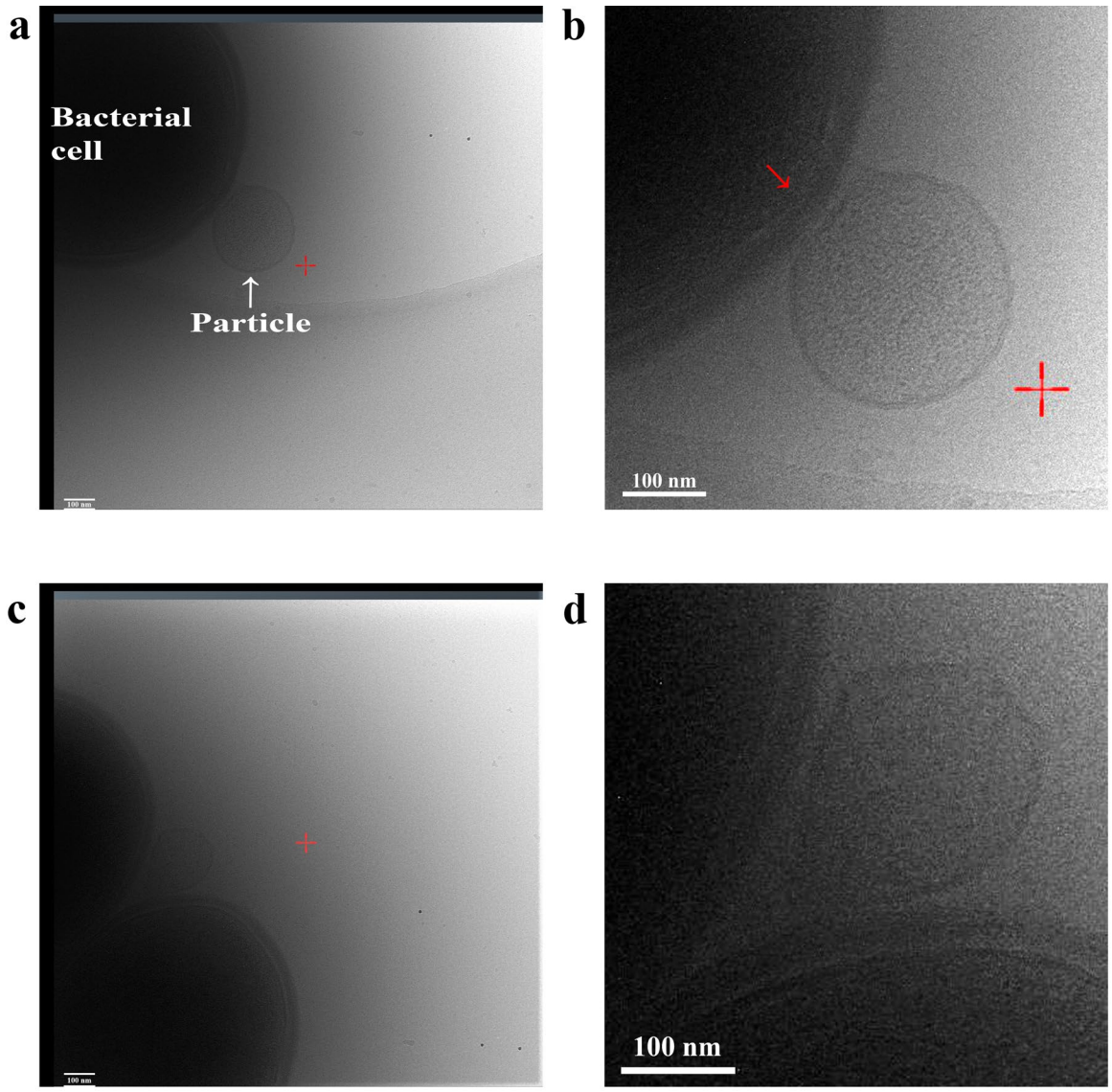

Figure 17. Cryo-EM-images taken of a solution of S. aureus that have been cultivated for 1 h together with AMP-modified particles. The scalebars are 100 nm in all images. The brightness has been adjusted in the images for better clarity. b) is a zoomed in image of a), and d) is a zoomed in image of c). The red arrow indicates an area where possible distortion in the membrane is visible (the red cross is a burned-in graphic, please disregard this).

4.4. Proteolytic stability

To analyze the stability against proteolytic degradation, the hydrogel discs of Paper 1 was placed in 20% serum and was removed from the serum at regular intervals, washed, and then cultivated for 24 h with *S. aureus*. The surfaces of the hydrogel discs were analyzed by LIVE/DEAD staining and the fraction of dead bacterial cells are presented in Figure 18. It was clear that the activity was maintained for the first 10 hours and that it was less active after 1 and 2 days in serum, but still showing an effect. The control and AMP-modified surfaces looked identical after 5 days, which indicates that somewhere between 2 and 5 days the peptides were degraded to such an extent where no antibacterial potency were present. These results show that by attaching the AMPs to LLCs of a hydrogel, the peptides maintain antibacterial activity for at least two days in 20% serum, which is a considerable higher lifetime compared to the AMPs of the innate immune system [71-73]. However, if the hydrogels were to be used in a wound dressing it is important to keep in mind that a change of dressing is necessary if antibacterial effect is to be maintained for longer durations.

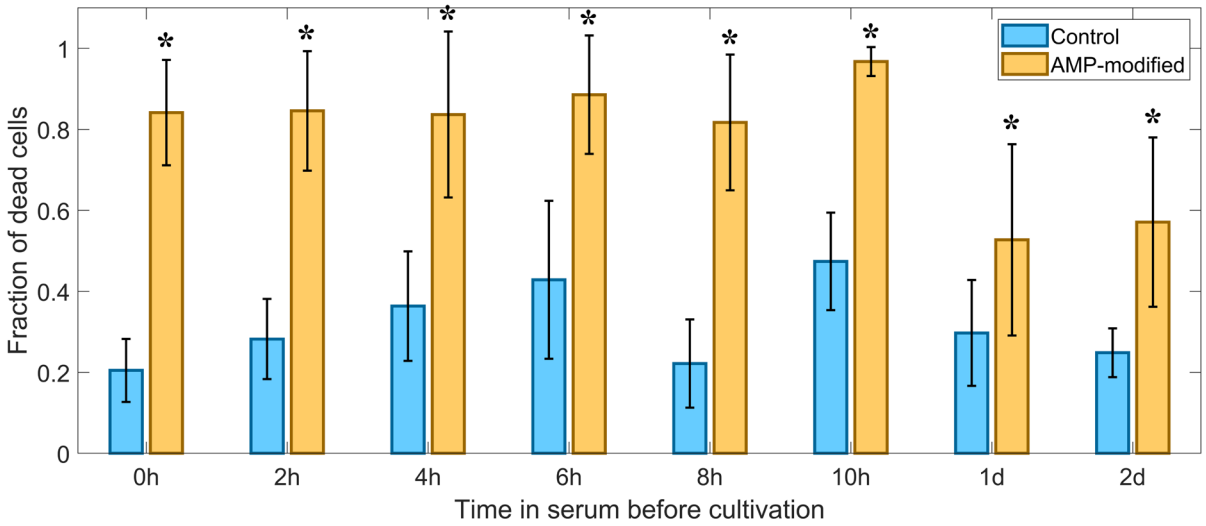

*Figure 18. The proportion of dead S. aureus on top of control and AMP-modified hydrogel surfaces after 24 h cultivation. The hydrogels were incubated in 20% serum prior to the cultivation with bacteria and taken out from the serum and washed with water according to the times on the x-axis. n=4 and the error bars are the standard deviation for the images taken of all samples. * indicates a significant difference compared to control of same time point, p<0.05.*

4.5. Cytotoxicity

The cytotoxicity of the hydrogels developed in Paper 1 was evaluated by an MTT assay against primary human dermal fibroblasts. The result from this test is presented in Figure 19. The cells cultivated in the sample exposed media from both the control and AMP-modified samples had a significantly higher viability over the 70% cut-off (substances that cause a viability less than

70% is considered to be cytotoxic). No difference was found in between the two hydrogel types. While there was a significantly higher standard deviation observed for the samples, the average viability was just a few percent lower than that of the negative control (cells cultivated in pure media). This test strongly indicates that no substances are leaching out from the materials at toxic levels during the three days of extraction.

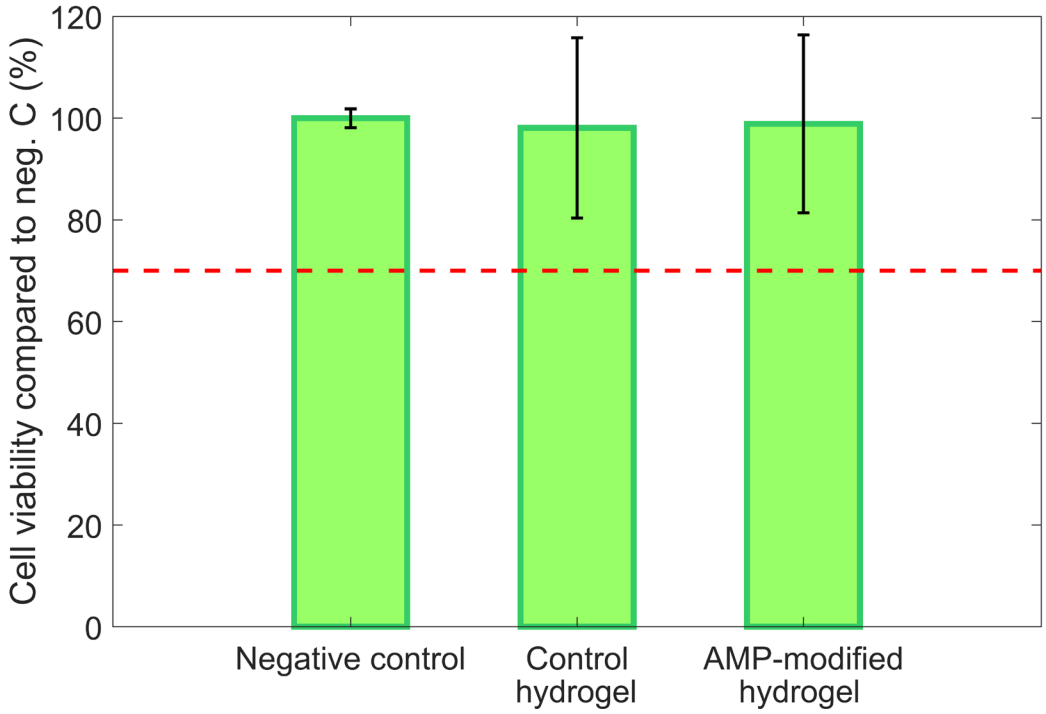

Figure 19. The cell viability of primary human dermal fibroblasts cultivated in sample exposed media compared to the negative control (cells in pure media). The red striped line indicates 70% cell viability, and the error bars are the standard deviation of n=8 samples. Both hydrogels tested was significantly higher than the 70% cut-off, $p<0.05$

4.6. Pilot *in vivo* study

The results from the pilot *in vivo* study are presented in Figure 20. Although the results support the overall hypothesis of the antibacterial activity of the materials, given the small scale of the study, the results need to be verified in large scale studies. However, the trend for the pilot study showed that the bacteria found on the implanted hydrogels were lower for both starting concentrations at both time intervals. This indicates that the AMP-modified hydrogels maintained their antibacterial activity even when implanted in rats. The results from the exudate were not as straight forward. The 24 hour evaluation with a 10^4 CFU/ml starting concentration showed higher CFU/ml for the AMP-modified hydrogel compared to the control. However, with a higher starting concentration ($2*10^6$ CFU/ml) there was a reduction in bacteria

for the AMP-modified hydrogels. To study the effect of AMP-modified hydrogels on the surrounding *in vivo* environment further studies are required.

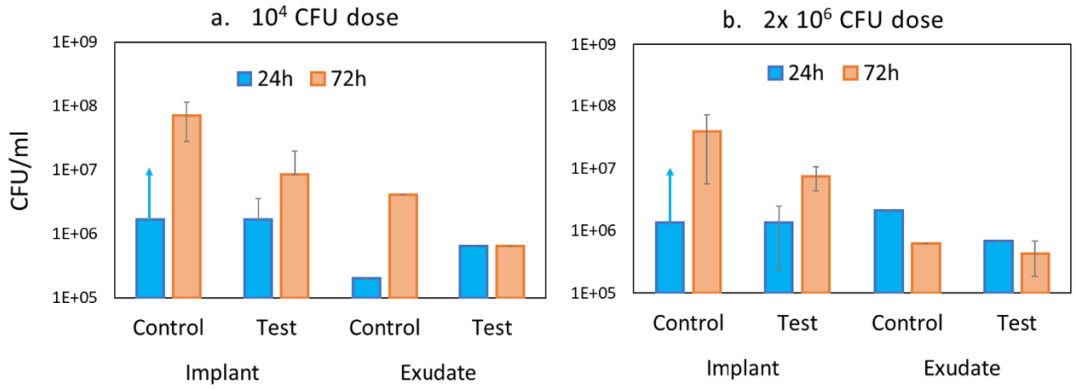

Figure 20. Results for the CFU/ml from the pilot in vivo study. (a) shows the results from the pockets with a starting concentration of 10^4 CFU/ml. (b) shows the results from the pockets with a starting concentration of $2*10^6$ CFU/ml. The 'control' is the non-modified hydrogels, and the 'test' is the AMP-modified samples. The blue arrow of the 24 h control samples means that the agar plates had a too high bacterial load to count individual colonies for the dilutions used.

5. Concluding remarks

The work presented in this thesis has shown two approaches to develop antibacterial materials consisting of cross-linked lyotropic liquid crystals with covalently attached antimicrobial peptides. The first concept is built on soft hydrogel sheets/discs that consists of 90 wt% water, which translated to a wound dressing would provide a wound with a moist environment while also lowering the bioburden. The results demonstrated that antibacterial effect against clinically relevant strains and even antibiotic resistant strains were achieved. By covalently attaching the antimicrobial peptides to the material they gained a protection against proteolytic degradation. This was demonstrated as antimicrobial activity was maintained for up to two days in serum. The antibacterial efficacy was achieved without causing cytotoxicity against primary human dermal fibroblasts, an important cell in the wound healing process.

The second concept is built on further increasing the antibacterial effect while also providing the potential of using an antibacterial liquid formulation, that offers a higher surface area and the potential to be used for deeper or harder to treat wounds. This was achieved by processing the cross-linked lyotropic liquid crystals into particles with a broad size distribution that was again modified with antimicrobial peptides. The micellar cubic structure was maintained throughout the procedure and the peptides were shown to covalently attach to the particles. Minimum inhibitory concentration-studies showed that a good antibacterial effect was achieved against both the gram-negative *E. coli* and the gram-positive *S. aureus*. In a higher concentrated slurry, a great reduction of bacterial load was observed in an agar plate model. This could provide a wound with a great protection against infection. Furthermore, cryo-EM studies indicated that the particles exerted their antibacterial effect by strongly interacting with the bacterial cell wall/membrane.

Both concepts showed a good antibacterial effect without using traditional antibiotics. More research like this will hopefully contribute to the development of new treatments that will get the upper hand in the battle against bacterial infections and antibiotic resistance.

6. Future perspectives

So far, the work has been focused on only one peptide. It would be of great interest to evaluate other peptides with the same LLC base. Furthermore, the work has only looked into one type of microbe – bacteria – as this is most relevant for wound infections. AMPs are however known to also be effective against some fungi and some enveloped viruses. It would therefore be of outmost interest to see what – if any – the effect against these microbes might be and how it might work.

Some AMPs are also known to activate certain parts of the wound healing process. It would therefore be of interest to perform further studies to investigate if the materials developed in this thesis can be used also for improving the wound healing. Along these lines it would also be of interest to investigate if the AMP-modified LLCs could also be used for drug administration for a dual benefit.

Finally, it would be a great benefit to have better control of the size of particles that were developed in this thesis. So far, a very rough top-down approach has been used to make the particles. It may be possible to utilize a more bottom-up approach to at least make particles of smaller sizes. This could for instance ease the hunt for interaction with bacteria as was observed with cryo-EM.

7. References

1. Holmqvist, P., P. Alexandridis, and B. Lindman, *Modification of the microstructure in poloxamer block copolymer− water−"oil" systems by varying the "oil" type.* Macromolecules, 1997. **30**(22): p. 6788-6797.
2. Robertson, A., et al., *DNA repair in mammalian cells.* Cellular and molecular life sciences, 2009. **66**(6): p. 981-993.
3. Risau, W., *Mechanisms of angiogenesis.* Nature, 1997. **386**(6626): p. 671-674.
4. McGrath, J., R. Eady, and F. Pope, *Anatomy and organization of human skin.* Rook's textbook of dermatology, 2004. **1**: p. 3.2-3.80.
5. Trommer, H. and R. Neubert, *Overcoming the stratum corneum: the modulation of skin penetration.* Skin pharmacology and physiology, 2006. **19**(2): p. 106-121.
6. Daly, C.H., *Biomechanical properties of dermis.* Journal of Investigative Dermatology, 1982. **79**(1): p. 17-20.
7. Nusgens, B., et al., *Collagen biosynthesis by cells in a tissue equivalent matrix in vitro.* Collagen and related research, 1984. **4**(5): p. 351-363.
8. Aderem, A. and D.M. Underhill, *Mechanisms of phagocytosis in macrophages.* Annual review of immunology, 1999. **17**(1): p. 593-623.
9. Metcalfe, D.D., D. Baram, and Y.A. Mekori, *Mast cells.* Physiological reviews, 1997.
10. Ezure, T. and S. Amano, *Influence of subcutaneous adipose tissue mass on dermal elasticity and sagging severity in lower cheek.* Skin Research and Technology, 2010. **16**(3): p. 332-338.
11. Jayakumar, R., et al., *Biomaterials based on chitin and chitosan in wound dressing applications.* Biotechnology advances, 2011. **29**(3): p. 322-337.
12. Wolberg, A.S. and R.A. Campbell, *Thrombin generation, fibrin clot formation and hemostasis.* Transfusion and Apheresis Science, 2008. **38**(1): p. 15-23.
13. Koh, T.J. and L.A. DiPietro, *Inflammation and wound healing: the role of the macrophage.* Expert reviews in molecular medicine, 2011. **13**.
14. Nissen, N.N., et al., *Vascular endothelial growth factor mediates angiogenic activity during the proliferative phase of wound healing.* The American journal of pathology, 1998. **152**(6): p. 1445.
15. Nissen, N.N., et al., *Basic fibroblast growth factor mediates angiogenic activity in early surgical wounds.* Surgery, 1996. **119**(4): p. 457-465.
16. Li, J., J. Chen, and R. Kirsner, *Pathophysiology of acute wound healing.* Clinics in dermatology, 2007. **25**(1): p. 9-18.
17. Vowden, K. and P. Vowden, *Wound dressings: principles and practice.* Surgery (Oxford), 2017. **35**(9): p. 489-494.
18. Madaghiele, M., et al., *Polymeric hydrogels for burn wound care: Advanced skin wound dressings and regenerative templates.* Burns & trauma, 2014. **2**(4): p. 2321-3868.143616.
19. Unnithan, A.R., et al., *Wound-dressing materials with antibacterial activity from electrospun polyurethane–dextran nanofiber mats containing ciprofloxacin HCl.* Carbohydrate polymers, 2012. **90**(4): p. 1786-1793.
20. Yari, A., H. Yeganeh, and H. Bakhshi, *Synthesis and evaluation of novel absorptive and antibacterial polyurethane membranes as wound dressing.* Journal of Materials Science: Materials in Medicine, 2012. **23**(9): p. 2187-2202.
21. Ong, S.-Y., et al., *Development of a chitosan-based wound dressing with improved hemostatic and antimicrobial properties.* Biomaterials, 2008. **29**(32): p. 4323-4332.

22. Kondo, S. and Y. Kuroyanagi, *Development of a wound dressing composed of hyaluronic acid and collagen sponge with epidermal growth factor.* Journal of Biomaterials Science, Polymer Edition, 2012. **23**(5): p. 629-643.
23. Xie, Z., et al., *Dual growth factor releasing multi-functional nanofibers for wound healing.* Acta biomaterialia, 2013. **9**(12): p. 9351-9359.
24. Doillon, C.J. and F.H. Silver, *Collagen-based wound dressing: Effects of hyaluronic acid and firponectin on wound healing.* Biomaterials, 1986. **7**(1): p. 3-8.
25. Lin, W.-C., et al., *Bacterial cellulose and bacterial cellulose–chitosan membranes for wound dressing applications.* Carbohydrate polymers, 2013. **94**(1): p. 603-611.
26. Thursby, E. and N. Juge, *Introduction to the human gut microbiota.* Biochemical Journal, 2017. **474**(11): p. 1823-1836.
27. Chen, Y.E., M.A. Fischbach, and Y. Belkaid, *Skin microbiota–host interactions.* Nature, 2018. **553**(7689): p. 427-436.
28. Baker-Austin, C. and J.D. Oliver, *Vibrio vulnificus: new insights into a deadly opportunistic pathogen.* Environmental microbiology, 2018. **20**(2): p. 423-430.
29. Church, D., et al., *Burn wound infections.* Clinical microbiology reviews, 2006. **19**(2): p. 403-434.
30. Giacometti, A., et al., *Epidemiology and microbiology of surgical wound infections.* Journal of clinical microbiology, 2000. **38**(2): p. 918-922.
31. Cogen, A., V. Nizet, and R. Gallo, *Skin microbiota: a source of disease or defence?* British Journal of Dermatology, 2008. **158**(3): p. 442-455.
32. Vivier, E., et al., *Innate or adaptive immunity? The example of natural killer cells.* science, 2011. **331**(6013): p. 44-49.
33. Murray, P.J. and T.A. Wynn, *Protective and pathogenic functions of macrophage subsets.* Nature reviews immunology, 2011. **11**(11): p. 723-737.
34. Iwasaki, A. and R. Medzhitov, *Regulation of adaptive immunity by the innate immune system.* science, 2010. **327**(5963): p. 291-295.
35. Kohanski, M.A., et al., *A common mechanism of cellular death induced by bactericidal antibiotics.* Cell, 2007. **130**(5): p. 797-810.
36. Davies, J. and D. Davies, *Origins and evolution of antibiotic resistance.* Microbiology and molecular biology reviews, 2010. **74**(3): p. 417-433.
37. Von Wintersdorff, C.J., et al., *Dissemination of antimicrobial resistance in microbial ecosystems through horizontal gene transfer.* Frontiers in microbiology, 2016. **7**: p. 173.
38. Wang, T., et al., *Hydrogel sheets of chitosan, honey and gelatin as burn wound dressings.* Carbohydrate polymers, 2012. **88**(1): p. 75-83.
39. Willix, D., P.C. Molan, and C. Harfoot, *A comparison of the sensitivity of wound-infecting species of bacteria to the antibacterial activity of manuka honey and other honey.* Journal of applied bacteriology, 1992. **73**(5): p. 388-394.
40. Kędziora, A., et al., *Similarities and differences between silver ions and silver in nanoforms as antibacterial agents.* International journal of molecular sciences, 2018. **19**(2): p. 444.
41. Jain, J., et al., *Silver nanoparticles in therapeutics: development of an antimicrobial gel formulation for topical use.* Molecular Pharmaceutics, 2009. **6**(5): p. 1388-1401.
42. Vankar, P.S. and D. Shukla, *Biosynthesis of silver nanoparticles using lemon leaves extract and its application for antimicrobial finish on fabric.* Applied Nanoscience, 2012. **2**(2): p. 163-168.
43. Chen, X. and H.J. Schluesener, *Nanosilver: a nanoproduct in medical application.* Toxicology letters, 2008. **176**(1): p. 1-12.

44. McShan, D., P.C. Ray, and H. Yu, *Molecular toxicity mechanism of nanosilver.* Journal of food and drug analysis, 2014. **22**(1): p. 116-127.
45. Zasloff, M., *Antimicrobial peptides of multicellular organisms.* nature, 2002. **415**(6870): p. 389-395.
46. Shai, Y., *Mode of action of membrane active antimicrobial peptides.* Peptide Science: Original Research on Biomolecules, 2002. **66**(4): p. 236-248.
47. Xu, L., et al., *Conversion of broad-spectrum antimicrobial peptides into species-specific antimicrobials capable of precisely targeting pathogenic bacteria.* Scientific Reports, 2020. **10**(1): p. 1-9.
48. Nguyen, L.T., E.F. Haney, and H.J. Vogel, *The expanding scope of antimicrobial peptide structures and their modes of action.* Trends in biotechnology, 2011. **29**(9): p. 464-472.
49. Costa, F., et al., *Covalent immobilization of antimicrobial peptides (AMPs) onto biomaterial surfaces.* Acta biomaterialia, 2011. **7**(4): p. 1431-1440.
50. Nguyen, L.T., et al., *Serum stabilities of short tryptophan-and arginine-rich antimicrobial peptide analogs.* PloS one, 2010. **5**(9): p. e12684.
51. Risso, A., *Leukocyte antimicrobial peptides: multifunctional effector molecules of innate immunity.* Journal of leukocyte biology, 2000. **68**(6): p. 785-792.
52. Hamamoto, K., et al., *Antimicrobial activity and stability to proteolysis of small linear cationic peptides with D-amino acid substitutions.* Microbiology and immunology, 2002. **46**(11): p. 741-749.
53. Wang, N., et al., *Nisin-loaded polydopamine/hydroxyapatite composites: Biomimetic synthesis, and in vitro bioactivity and antibacterial activity evaluations.* Colloids and Surfaces A: Physicochemical and Engineering Aspects, 2020: p. 125101.
54. Nordström, R. and M. Malmsten, *Delivery systems for antimicrobial peptides.* Advances in colloid and interface science, 2017. **242**: p. 17-34.
55. Hilpert, K., et al., *Screening and characterization of surface-tethered cationic peptides for antimicrobial activity.* Chemistry & biology, 2009. **16**(1): p. 58-69.
56. Bagheri, M., M. Beyermann, and M. Dathe, *Immobilization reduces the activity of surface-bound cationic antimicrobial peptides with no influence upon the activity spectrum.* Antimicrobial agents and chemotherapy, 2009. **53**(3): p. 1132-1141.
57. Gabriel, M., et al., *Preparation of LL-37-grafted titanium surfaces with bactericidal activity.* Bioconjugate chemistry, 2006. **17**(2): p. 548-550.
58. Soares, J.W., et al., *Immobilization and orientation-dependent activity of a naturally occurring antimicrobial peptide.* Journal of Peptide Science, 2015. **21**(8): p. 669-679.
59. Li, Y., et al., *Effects of peptide immobilization sites on the structure and activity of surface-tethered antimicrobial peptides.* The Journal of Physical Chemistry C, 2015. **119**(13): p. 7146-7155.
60. Diniz, I.M., et al., *Pluronic F-127 hydrogel as a promising scaffold for encapsulation of dental-derived mesenchymal stem cells.* Journal of Materials Science: Materials in Medicine, 2015. **26**(3): p. 153.
61. Schmolka, I.R., *Artificial skin I. Preparation and properties of pluronic F-127 gels for treatment of burns.* Journal of biomedical materials research, 1972. **6**(6): p. 571-582.
62. Müller, M., et al., *Nanostructured Pluronic hydrogels as bioinks for 3D bioprinting.* Biofabrication, 2015. **7**(3): p. 035006.
63. Vandenhaute, M., et al., *Stability of Pluronic® F127 bismethacrylate hydrogels: Reality or utopia?* Polymer Degradation and Stability, 2017. **146**: p. 201-211.
64. Lacoste, J. and D. Carlsson, *Gamma-, photo-, and thermally-initiated oxidation of linear low density polyethylene: A quantitative comparison of oxidation products.* Journal of Polymer Science Part A: Polymer Chemistry, 1992. **30**(3): p. 493-500.

65. Hu, H., et al., *Engineering of a novel pluronic F127/graphene nanohybrid for pH responsive drug delivery.* Journal of biomedical materials research Part A, 2012. **100**(1): p. 141-148.
66. Desai, S.D. and J. Blanchard, *In vitro evaluation of pluronic F127-based controlled-release ocular delivery systems for pilocarpine.* Journal of pharmaceutical sciences, 1998. **87**(2): p. 226-230.
67. Cutting, K.F. and R.J. White, *Maceration of the skin and wound bed 1: its nature and causes.* Journal of wound care, 2002. **11**(7): p. 275-278.
68. Khattak, S.F., S.R. Bhatia, and S.C. Roberts, *Pluronic F127 as a cell encapsulation material: utilization of membrane-stabilizing agents.* Tissue engineering, 2005. **11**(5-6): p. 974-983.
69. Holmqvist, P., P. Alexandridis, and B. Lindman, *Phase Behavior and Structure of Ternary Amphiphilic Block Copolymer− Alkanol− Water Systems: Comparison of Poly (ethylene oxide)/Poly (propylene oxide) to Poly (ethylene oxide)/Poly (tetrahydrofuran) Copolymers.* Langmuir, 1997. **13**(9): p. 2471-2479.
70. He, W.X., et al., *Mesoscopically Ordered Bone-Mimetic Nanocomposites.* Advanced Materials, 2015. **27**(13): p. 2260-2264.
71. Sharma, A., et al., *Designing of peptides with desired half-life in intestine-like environment.* BMC bioinformatics, 2014. **15**(1): p. 1-8.
72. Singh, D., R. Vaughan, and C.C. Kao, *LL-37 peptide enhancement of signal transduction by toll-like receptor 3 is regulated by pH.* Journal of Biological Chemistry, 2014. **289**(40): p. 27614-27624.
73. Mathur, D., et al., *PEPlife: a repository of the half-life of peptides.* Scientific reports, 2016. **6**(1): p. 1-7.